Supporting information

Phase control for indium oxide nanoparticles

Ida Gjerlevsen Nielsen, Sanna Sommer, Bo Brummerstedt Iversen*

Center for Materials Crystallography, Department of Chemistry and iNANO, Aarhus University,

8000 Aarhus C, Denmark

Contents

Reported indium oxide synthesis

Main solvent	T / °C	Pressure / MPa	Phase	Ref
H_2O	380	30	c-In_2O_3	[1]
H_2O	400	24.1	c-In_2O_3	[2]
H_2O	450	24	c-In_2O_3	[3]

Table S1. Previously reported flow synthesis.

Main solvent	T / °C	Time / h	Phase	Additive	Ref
Acetophenone	200	48	c-In_2O_3		[4]
Butanone	200	48	c-In_2O_3		[4]
Benzyl alcohol	200	48	c-In_2O_3		[4]
Benzyl amine	200	48	c-In_2O_3		[4]
Ethanol	RT-180	1-16	Amorp./ $In(OH)_3$/ InOOH /c-In_2O_3	PVP, CTAB, octane, H_2O	[5]
Ethanol	100-220	1-792	Amorp./ $In(OH)_3$/ InOOH /c-In_2O_3	NH_3, NaOH	[6]
Ethylenediamine	220	24	InOOH	H_2O	[7]
Ethylenediamine	180	24	$In(OH)_3$	H_2O	[7]
DMF	150	24	$In(OH)_3$/ InOOH/ c-In_2O_3	H_2O	[8]
PEG-400	210	24	InOOH/ c-In_2O_3	H_2O, HMDA	[9]

Table S2. Previously reported autoclave synthesis.

Main solvent	Additive	Phase	Calcination temp. / °C	Calcined to	Ref
H_2O	Urea	Amorp., $In(OH)_3$			[10]
H_2O	Urea	Amorp.	250	h-In_2O_3	[11]
H_2O	KI	$In(OH)_3$	250	h-In_2O_3	[11]
H_2O	KCl	$In(OH)_3$	250	c-In_2O_3	[11]
H_2O	NH_3	$In(OH)_3$	240	c-In_2O_3	[12]
H_2O	NH_3	$In(OH)_3$	250-500	c-In_2O_3	[13]
Methanol	NH_3	$In(OH)_3$	250-500	h-In_2O_3	[13]
Methanol	NaOH	InOOH	300-500	c-In_2O_3	[14]
EtOH	NaOH	InOOH	300-500	h-In_2O_3 - c-In_2O_3	[14]

Table S3. Previously reported synthesis at low temperature (RT-95 °C) by precipitation.

Experimental conditions and calibrations

Name	Solvent	Sample temperature / °C	Set temperatures / °C
E400	Ethanol	400	450
E275	Ethanol	275	280
ERamp1	Ethanol	100, 150, 200, 350, 400, 450	110, 175, 230, 400, 450, 500
ERamp2	Ethanol	200, 350	230, 400
W350	Water	350	400
W325	Water	325	350
W275	Water	275	300
WRamp	Water	100, 150, 200, 300, 350, 400, 450	110, 175, 230, 350, 400, 450, 500
WB450	Water + NaOH	450	464
WB350	Water + NaOH	350	360
WBRamp1	Water + NaOH	100, 150, 200, 350	100, 152, 204, 360
WBRamp2	Water + NaOH	100, 150, 200, 250, 300, 350	96, 151, 206, 261, 316, 371, 426

Table S4. Names, solvents and temperature of the *in situ* experiments. The experiments were conducted at three different beamtimes. For each a temperature calibration was done using a thermocouple to measure the temperature in the capillary at the beam position (T_{sample}). The correlation between the set temperature of the heater (T_{set}) and actual temperature for the three beamtimes are shown in Figure S2-4.

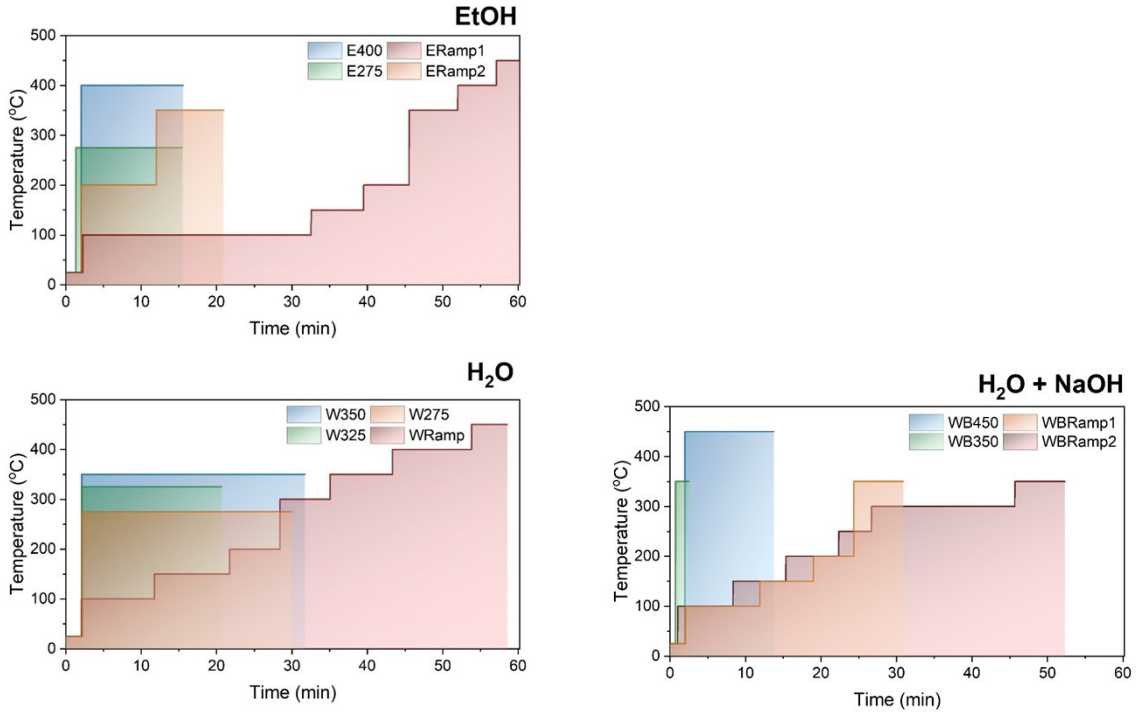

Figure S1. Temperature profiles of all *in situ* solvothermal synthesis.

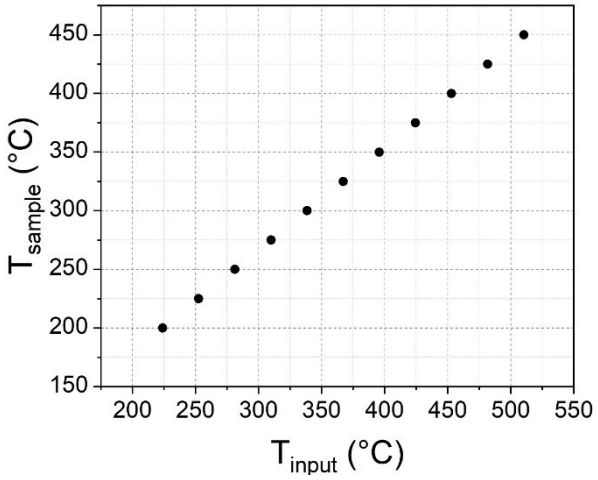

Figure S2. Temperature calibration used for E400, ERamp1, Eramp2, W275, W325, W350 and WRamp.

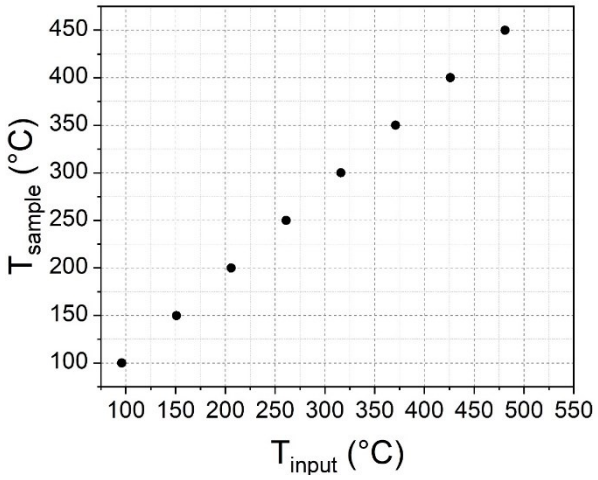

Figure S3. Temperature calibration for WBRamp2.

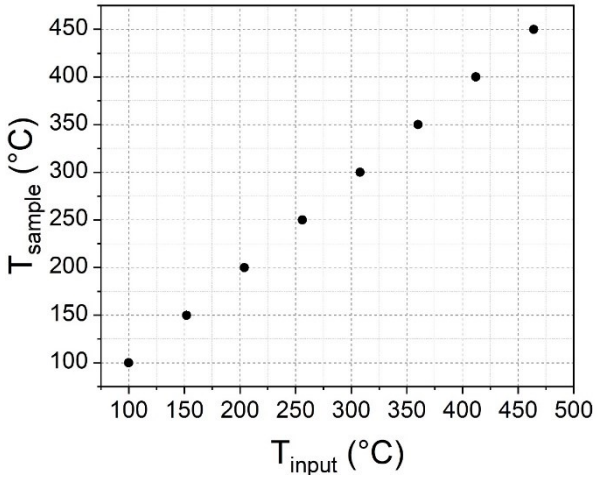

Figure S4. Temperature calibration for E275, WB450, WB350 and RRamp1.

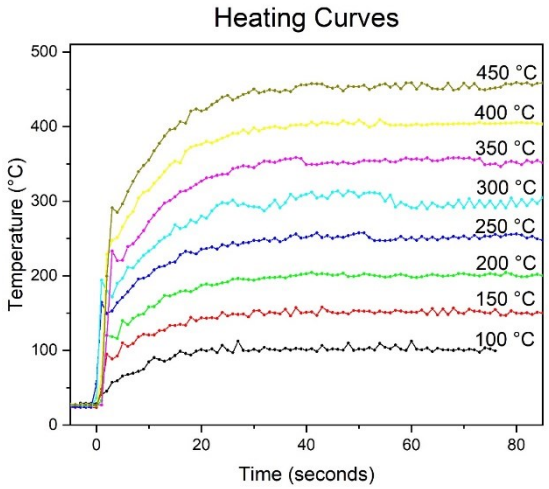

Figure S5. The heating rate for direct heating for E275, WB450, WB350 and RRamp1. The ramps for the experiments during other beamtimes are similar.

Concentration	Solvent	Temperatures / °C
0.01 M	Water	200, 325, 350, 375, 400, 425, 450
0.01 M	Ethanol	200, 250, 325, 350, 375, 400, 425, 450
0.1 M, 0.5 M, 1.0 M	Ethanol	350

Table S5. Conditions for the 18 samples synthesized by flow

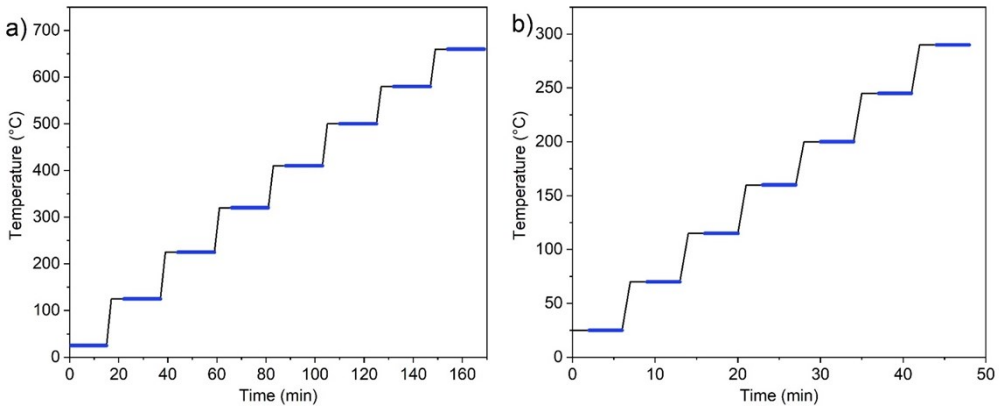

Figure S6. Heating profiles for the *in situ* calcination experiments. The blue intervals mark the measurement time. a) For InOOH synthesized in flow: Heating rate of 50 °C/min, 5 min temperature stabilization and 15 min exposure. b) For $In(OH)_3$ synthesized in autoclave: Heating rate of 50 °C/min, 2 min temperature stabilization and 2x2 min exposure. These were summed when no transformations occurred.

Supporting Information Experimental

Transmission electron microscopy (TEM) was conducted for the phase pure InOOH sample synthesized by flow synthesis at 325 °C. Images were acquired in bright field on a TALOS F200A with a TEIN lens system, X-FEG electron source and Ceta 16M Camera. The samples were placed on a Cu grid after dispersion in ethanol (99% purity).

Total scattering (TS) data was collected for the phase pure InOOH sample synthesized by flow synthesis at 325 °C. The conditions were the same as for the *in situ* experiments, except the sample was packed in a Kapton capillary with a diameter of 0.7 mm. Data analysis of the TS data was performed as described in the main article, with the background was scattering from a kapton capillary and q_{max}=23.5 Å.

TS data was also collected for samples made by adding 4 M aqueous NaOH to 1 M aqueous $In(NO_3)_3$ solutions. The samples had different ratio of In^{3+} to OH^- given by $r = [OH^-]/[In^{3+}]$. The samples had ratios of r = 0.6, 0.8, 1, 2, 3 and 4. Samples were contained in 1.0 mm Kapton capillaries, and data were collected for 2-5 min per sample. Data transformation was done with background measurements of water added an identical amount of NaOH as the sample. The transformation parameters deviating from the *in situ* data are q_{min} = 0.78 $Å^{-1}$ and q_{max} = 19-22 $Å^{-1}$. The PDFs were refined with the phase $In(OH)_3$, using only the parameters scale factor and size.

Phase identification and extracted parameters

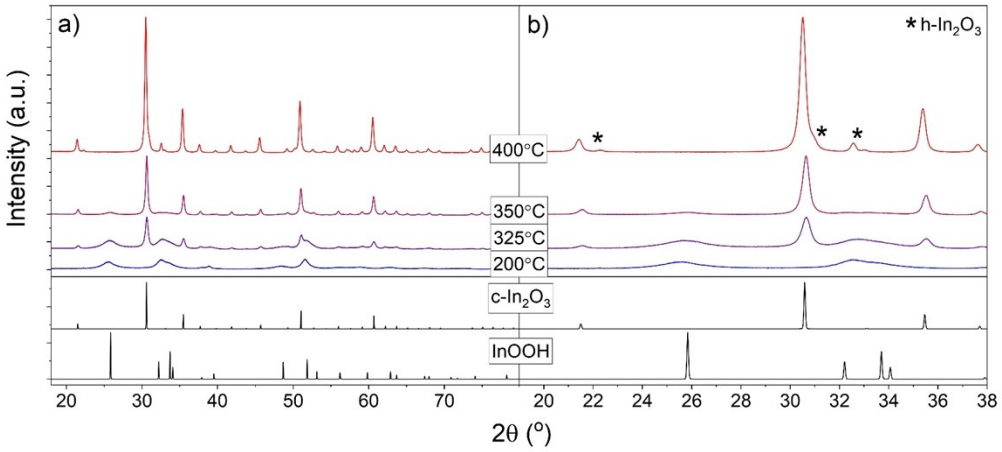

Figure S7. Selected diffractograms of samples synthesized by flow synthesis with ethanol as solvent. a) Full diffractograms, b) Zoom in showing the minor phases.

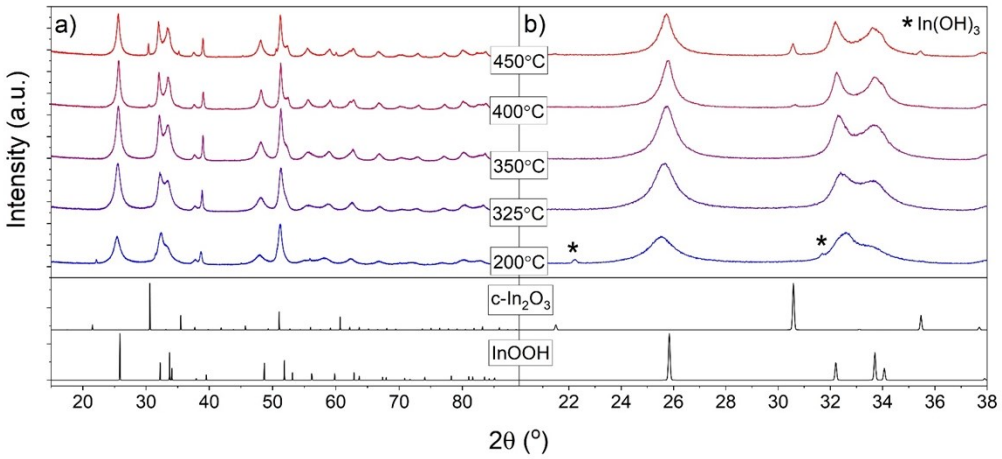

Figure S8. Selected diffractograms samples synthesized by flow synthesis with water as solvent. a) Full diffractograms, b) Zoom in showing the minor phases.

	c-In_2O_3			h-In_2O_3				InOOH					$In(OH)_3$			
	Scale	a	Size	Scale	a	c	Size	Scale	a	b	c	Size	Scale	a	Size	R_w
E400	0.470	10.114	107.5	-	-	-	-	-	-	-	-	-	-	-	-	0.275
E275	0.249	10.004	81.1	-	-	-	-	-	-	-	-	-	-	-	-	0.210
ERamp1	-	-	-	0.507	5.478	14.505	500^	0.0149	5.255*	4.57*	3.27*	70.7	-	-	-	0.275
ERamp2	0.530	10.078	129.8	-	-	-	-	0.0313	5.060	4.827	3.426	39.6	-	-	-	0.237
W350	0.668	10.258	79.23	-	-	-	-	9.45E-4	5.30*	4.67*	3.30*	50^	-	-	-	0.233
W325	0.217	10.22	78.5	-	-	-	-	0.0125	5.30*	4.67*	3.30*	50^	-	-	-	0.268
W275	0.581	10.233	78.22	-	-	-	-	0.0521	5.30*	4.67*	3.30*	96.3	-	-	-	0.265
WRamp	0.219	10.24	93.6	0.135	5.547	14.68	100.7	0.145	5.327*	4.64*	3.31*	199	-	-	-	0.320
WB450	-	-	-	-	-	-	-	0.162	5.209	4.520	3.234	69.93	0.00	7.81*	12.7*	0.321
WB350	-	-	-	-	-	-	-	0.194	5.197	4.519	3.232	115.5	0.014	7.74*	32.3*	0.318
WBRamp1	-	-	-	-	-	-	-	0.240	5.178	4.517	3.233	128.7	0.015	7.75*	20^	0.275

Table S6. Refined parameters from PDF analysis for the last frame for each *in situ* solvothermal experiment. *Parameter was fixed at this value, which was obtain from refinement of a frame with a higher signal. ^These sizes were fixed as not enough signal as present to refine them at similar conditions.

	InOOH					$In(OH)_3$						
	Scale	a	b	c	Y	Scale	a	I_G	R_p	R_{wp}	R_{exp}	χ^2
WBRamp2	2.85E-6	5.276	4.578	3.281	0.0657	9.44E-9	8.001*	0.0335	14.7	14.6	14.83	0.971

Table S7. Refined parameters from Rietvled refinement for the last frame in the *in situ* solvothermal experiment WBRamp2. *Parameter was fixed at this value, which was obtain from refinement of a frame with a higher signal.

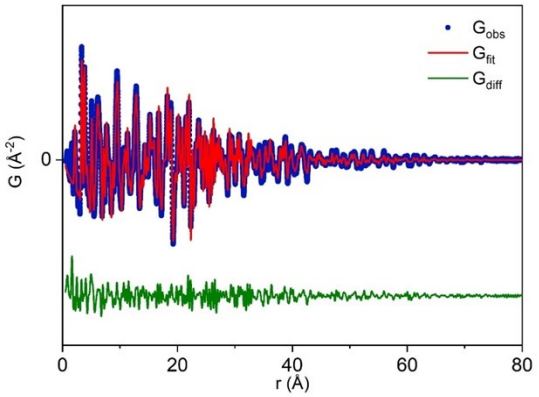

Figure S9. PDF analysis using phase pure c-In_2O_3 of the last frame for experiment E400.

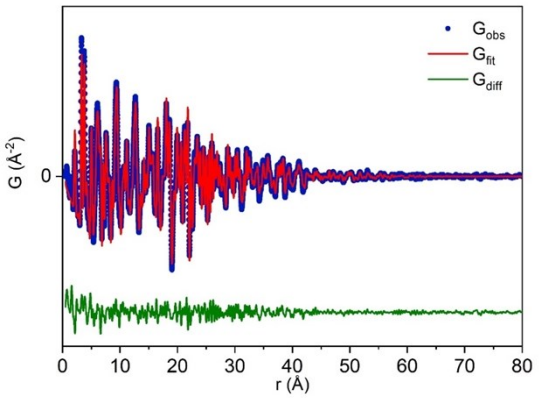

Figure S10. PDF analysis of the last frame for experiment E275 using phase pure c-In_2O_3.

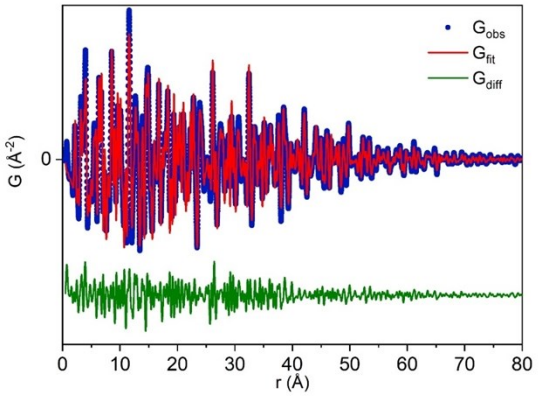

Figure S11. PDF analysis of the last frame for experiment ERamp1 using h-In_2O_3 and a limited amount of InOOH.

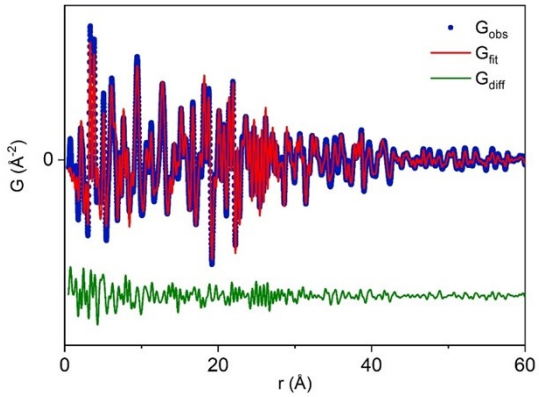

Figure S12. PDF analysis of the last frame for experiment ERamp2 using c-In_2O_3 and a limited amount of InOOH.

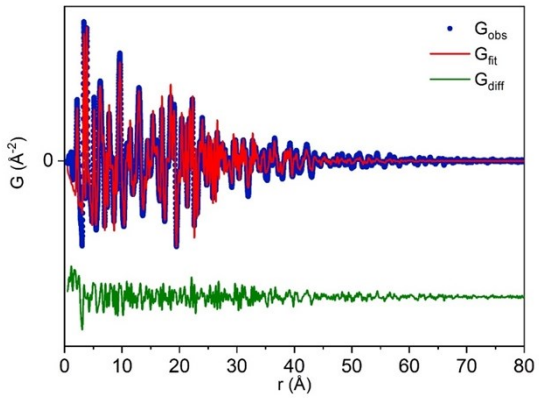

Figure S13. PDF analysis of the last frame for experiment W275 using c-In_2O_3 and a limited amount of InOOH.

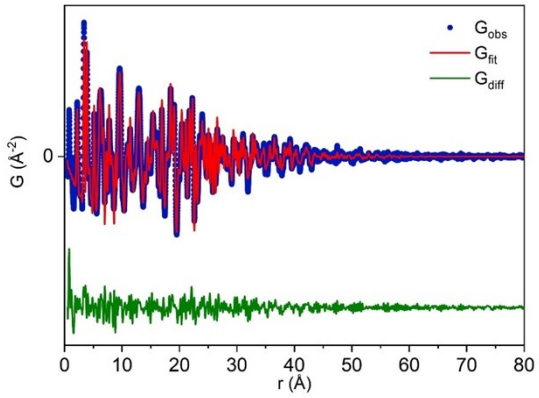

Figure S14. PDF analysis of the last frame for experiment W325 using c-In_2O_3 and a limited amount of InOOH.

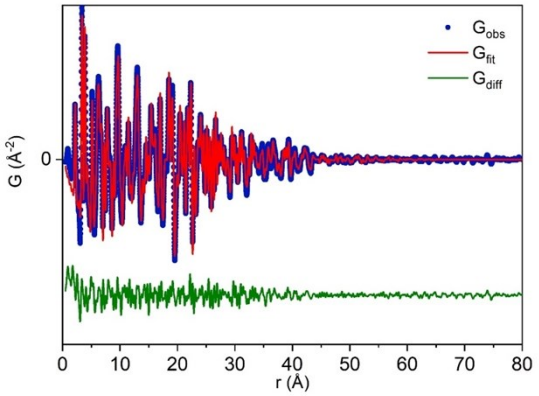

Figure S15. PDF analysis of the last frame for experiment W350 using c-In_2O_3 and a miniscule amount of InOOH.

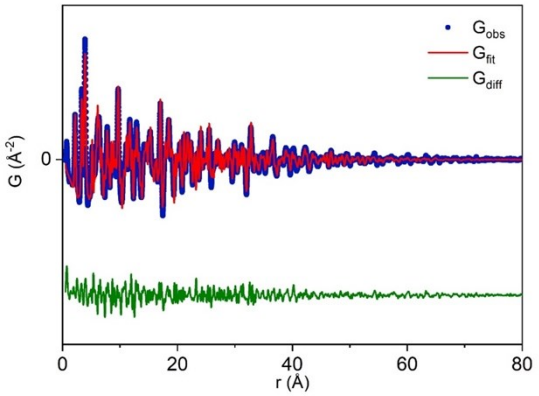

Figure S16. PDF analysis of the last frame for experiment WRamp using a mixture of c-In_2O_3, h-In_2O_3 and InOOH.

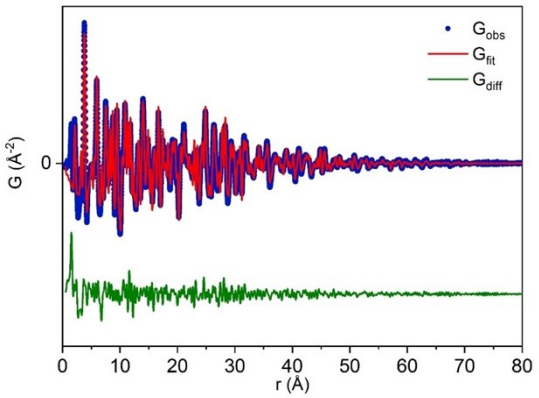

Figure S17. PDF analysis of the last frame for experiment WB350 using InOOH and a miniscule amount of $In(OH)_3$.

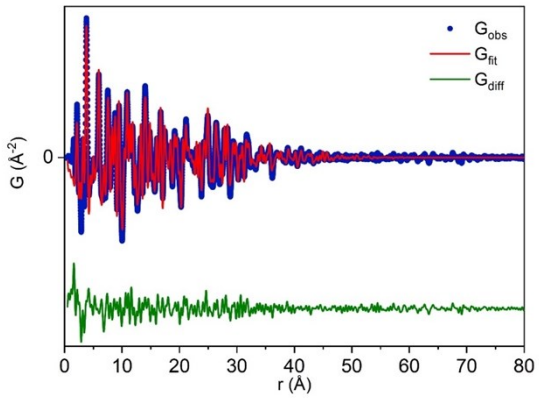

Figure S18. PDF analysis of the last frame for experiment WB450 using InOOH and a miniscule amount of $In(OH)_3$.

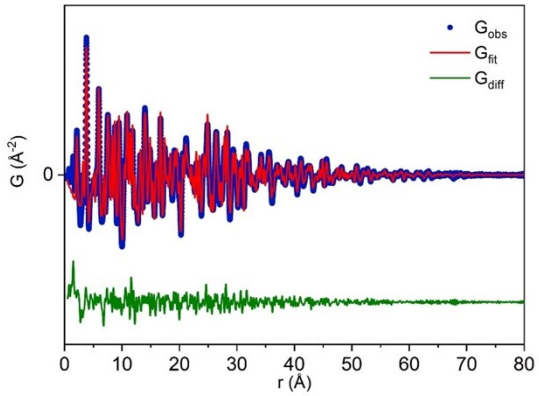

Figure S19. PDF analysis of the last frame for experiment WBRamp1 using InOOH and a miniscule amount of $In(OH)_3$.

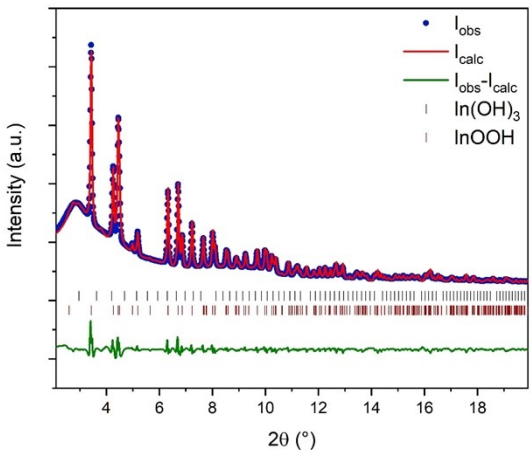

Figure S20. Rietveld fit of the last frame for experiment WBRamp2 using InOOH and a miniscule amount of $In(OH)_3$.

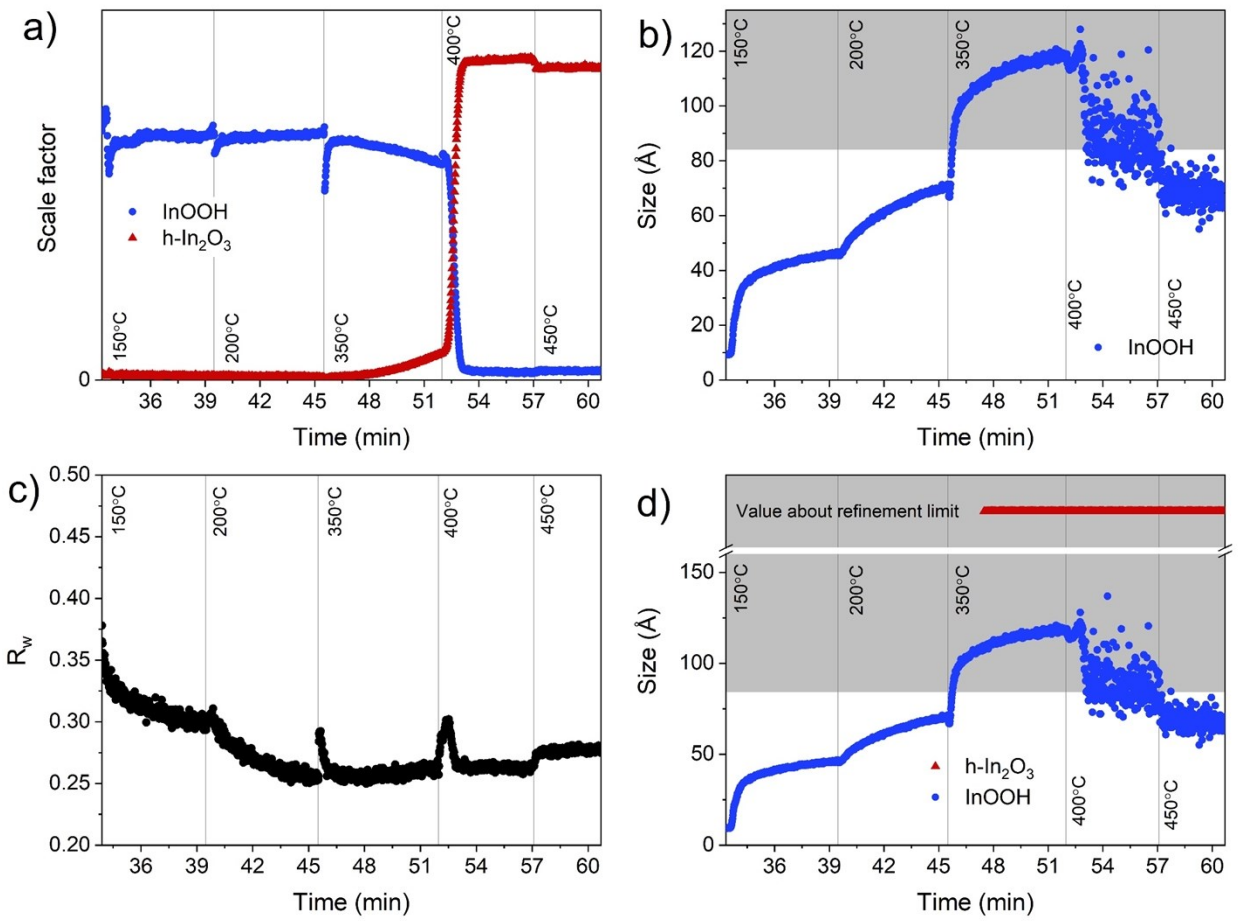

Figure S21. Extracted parameters from PDF analysis of ERamp1 (Solvent: Ethanol, Heating: Ramp with steps at 100, 150, 200, 350, 400 and 450 °C). a) Scale factors. b) Size for InOOH. c) R-value. d) The used size of h-In_2O_3 in the refinement compared to the extracted InOOH sizes. The size of the formed h-In_2O_3 was attempted refined, but the sizes were too large to reliably refine throughout the experiment. (The grey area marks the approximate resolution limit, as defined by Sommer *et al.*[15] as where the Q_{damp} and size functions intersect. For the Q_{damp}=0.0349 as used here, the resolution limit is 84 Å)

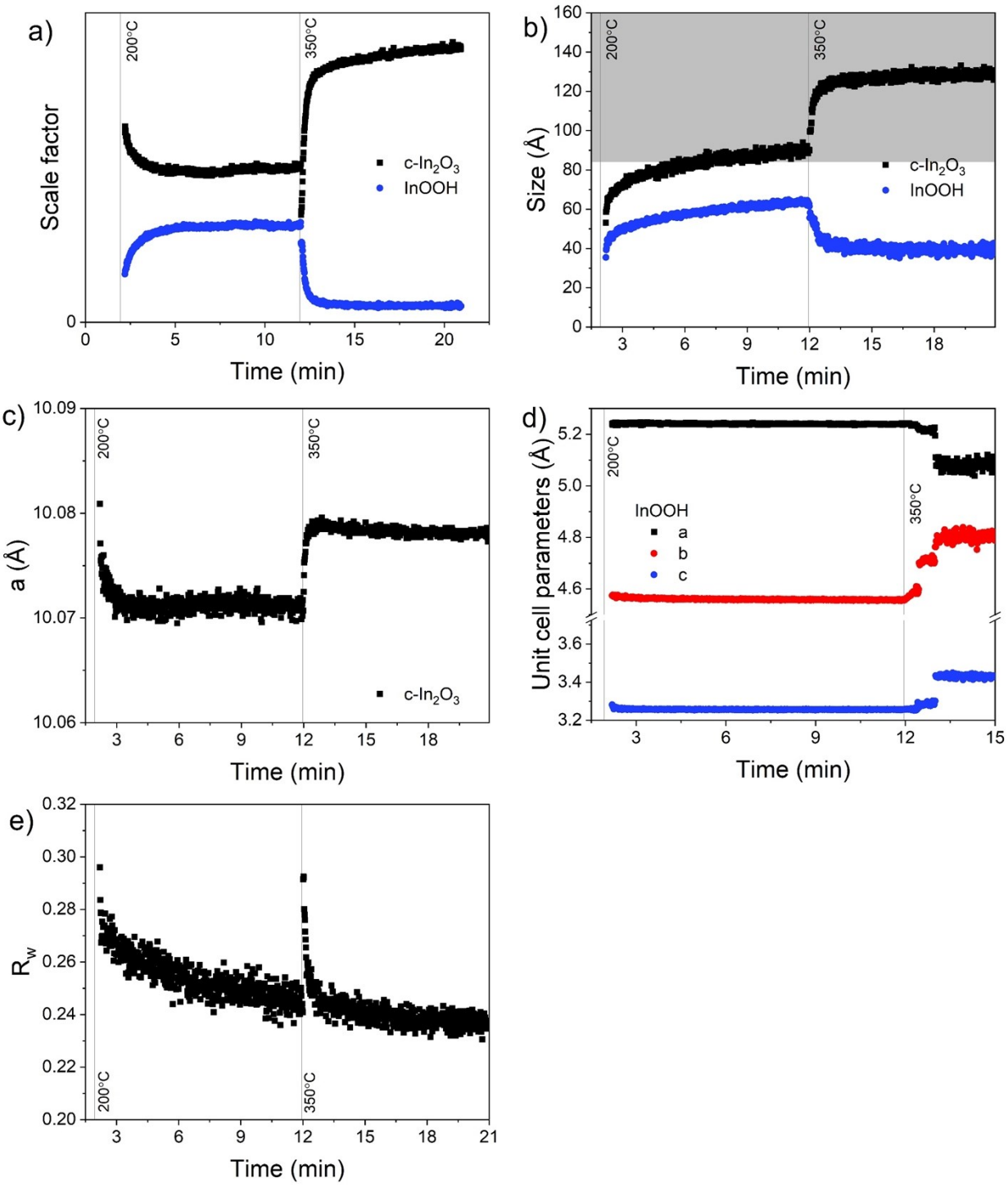

Figure S22. Extracted parameters from PDF analysis of ERamp2 (Solvent: Ethanol, Heating: Ramp with steps at 200 and 350 °C). a) Scale factors. b) Sizes (The grey area marks the approximate resolution limit, as defined by Sommer *et al.*[15] as where the Q_{damp} and size functions intersect. For the Q_{damp}=0.0349 as used here, the resolution limit is 84 Å). c) Unit cell parameter, a, for c-In_2O_3. d) Unit cell parameters, a, b and c, for InOOH. e) R-value.

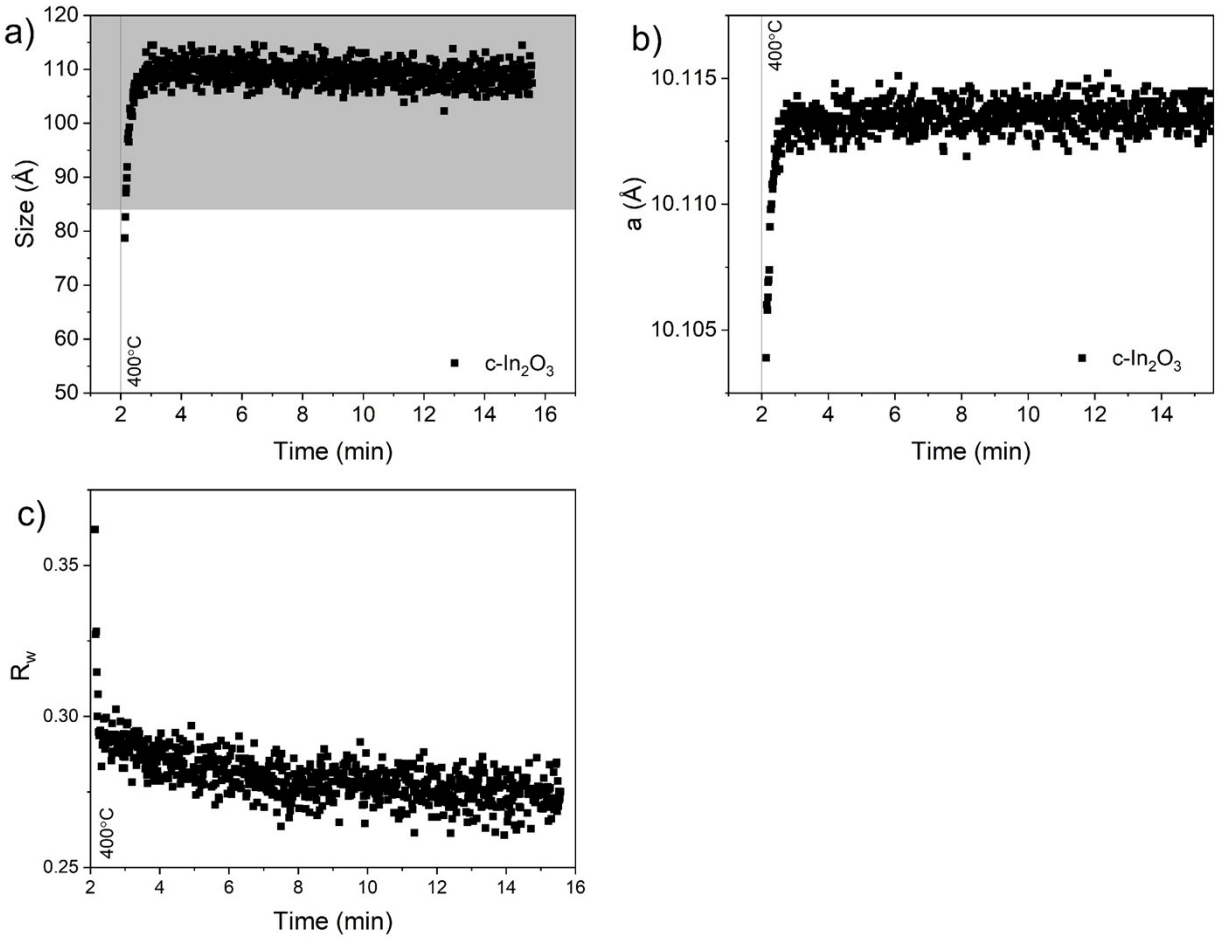

Figure S23. Extracted parameters from PDF analysis of experiment E400 (Solvent: Ethanol, Heating: Direct to 400 °C). a) Size (The grey area marks the approximate resolution limit, as defined by Sommer *et al.*[15] as where the Q_{damp} and size functions intersect. For the Q_{damp}=0.0349 as used here, the resolution limit is 84 Å). b) Unit cell parameter, a. c) R-value.

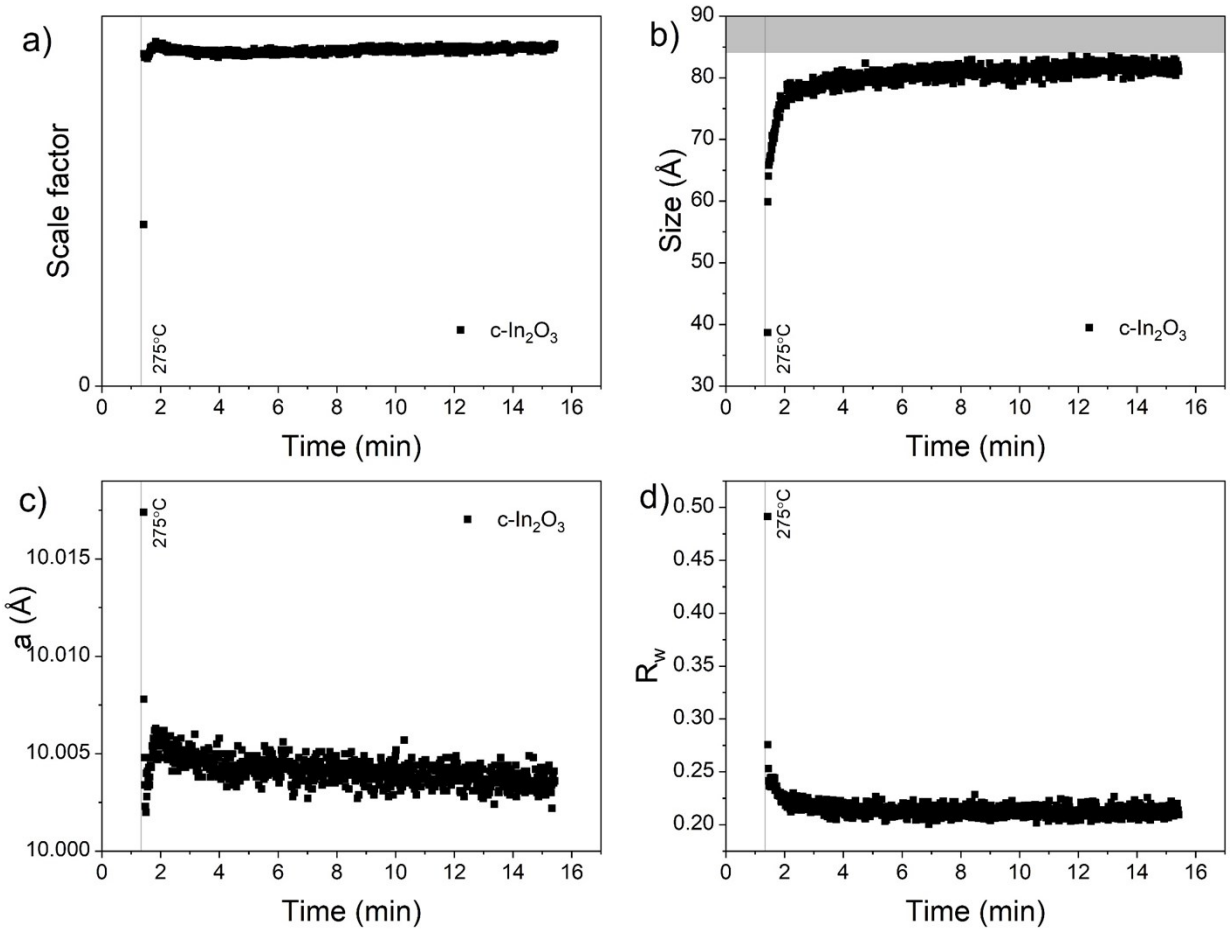

Figure S24. Extracted parameters from PDF analysis of experiment E275 (Solvent: Ethanol, Heating: Direct to 275 °C). a) Scale factor. b) Size (The grey area marks the approximate resolution limit, as defined by Sommer *et al.*[15] as where the Q_{damp} and size functions intersect. For the Q_{damp}=0.0349 as used here, the resolution limit is 84 Å). c) Unit cell parameter, a. d) R-value.

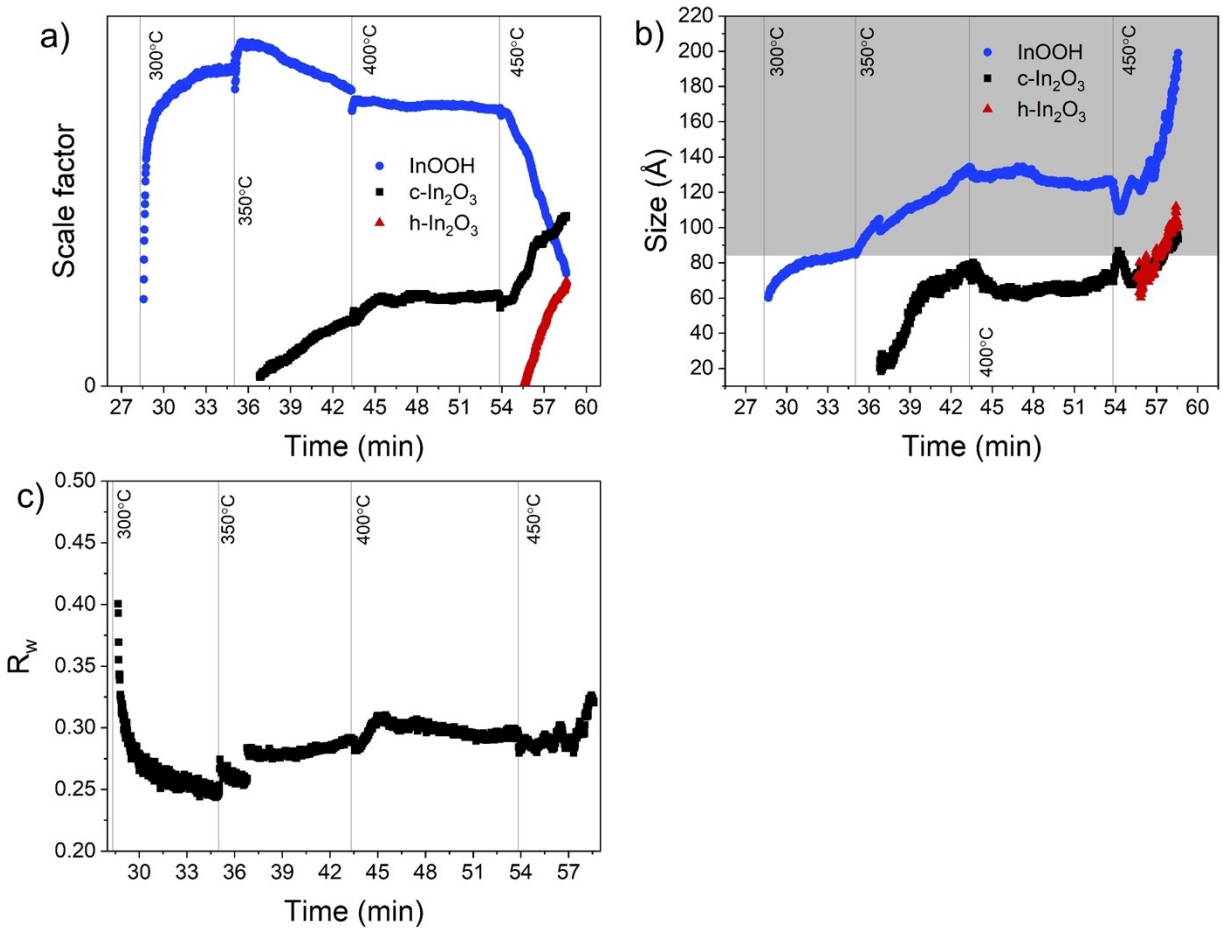

Figure S25. Extracted parameters from PDF analysis of WRamp (Solvent: Water, Heating: Ramp with steps at 100, 150, 200, 300, 350, 400 and 450 °C). a) Scale factors. b) Sizes. (The grey area marks the approximate resolution limit, as defined by Sommer *et al.*[15] as where the Q_{damp} and size functions intersect. For the Q_{damp}=0.0349 as used here, the resolution limit is 84 Å). c) R-value.

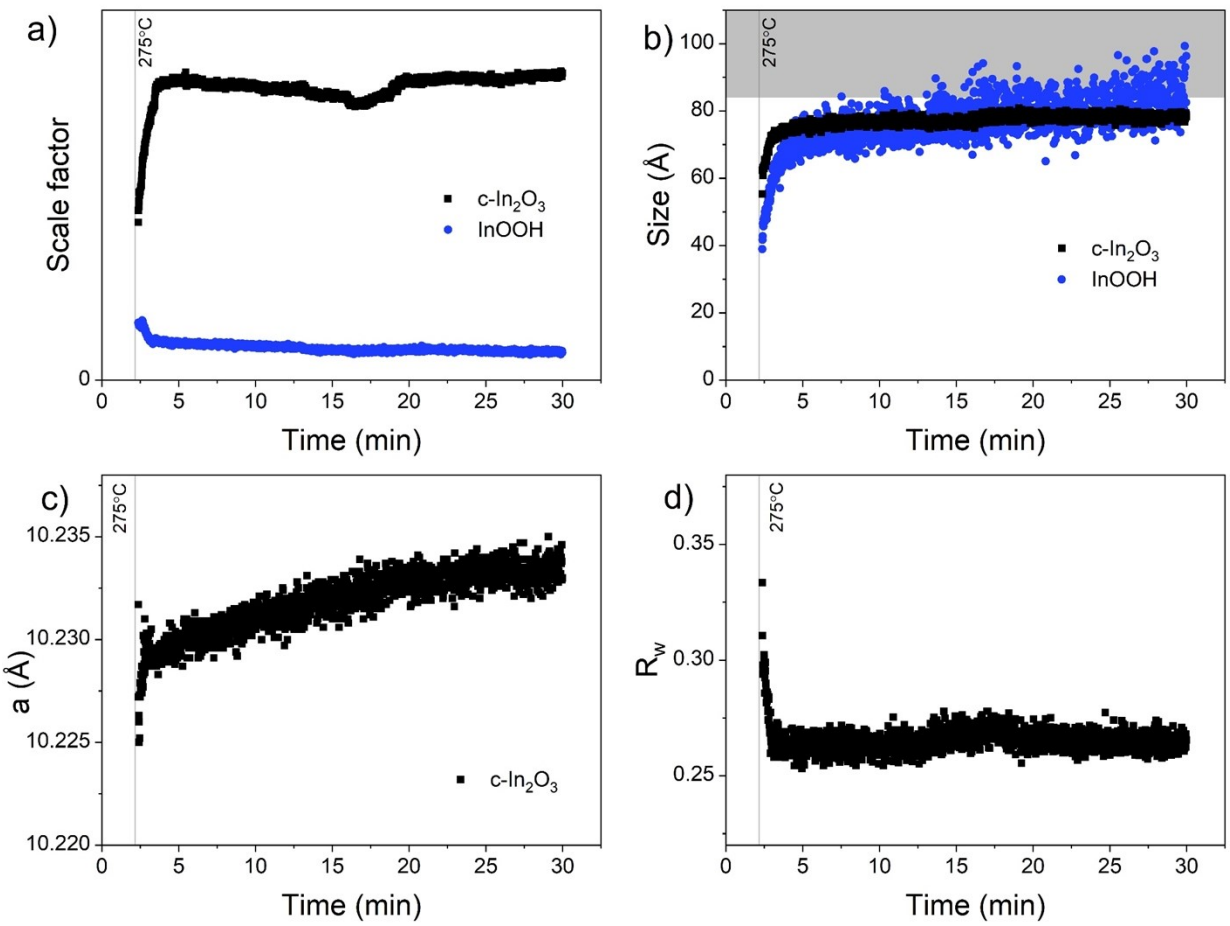

Figure S26. Extracted parameters from PDF analysis of W275 (Solvent: Water, Heating: Direct to 275 °C). a) Scale factors. b) Sizes (The grey area marks the approximate resolution limit, as defined by Sommer *et al*.[15] as where the Q_{damp} and size functions intersect. For the Q_{damp}=0.0349 as used here, the resolution limit is 84 Å). c) Unit cell parameter, a. d) R-value.

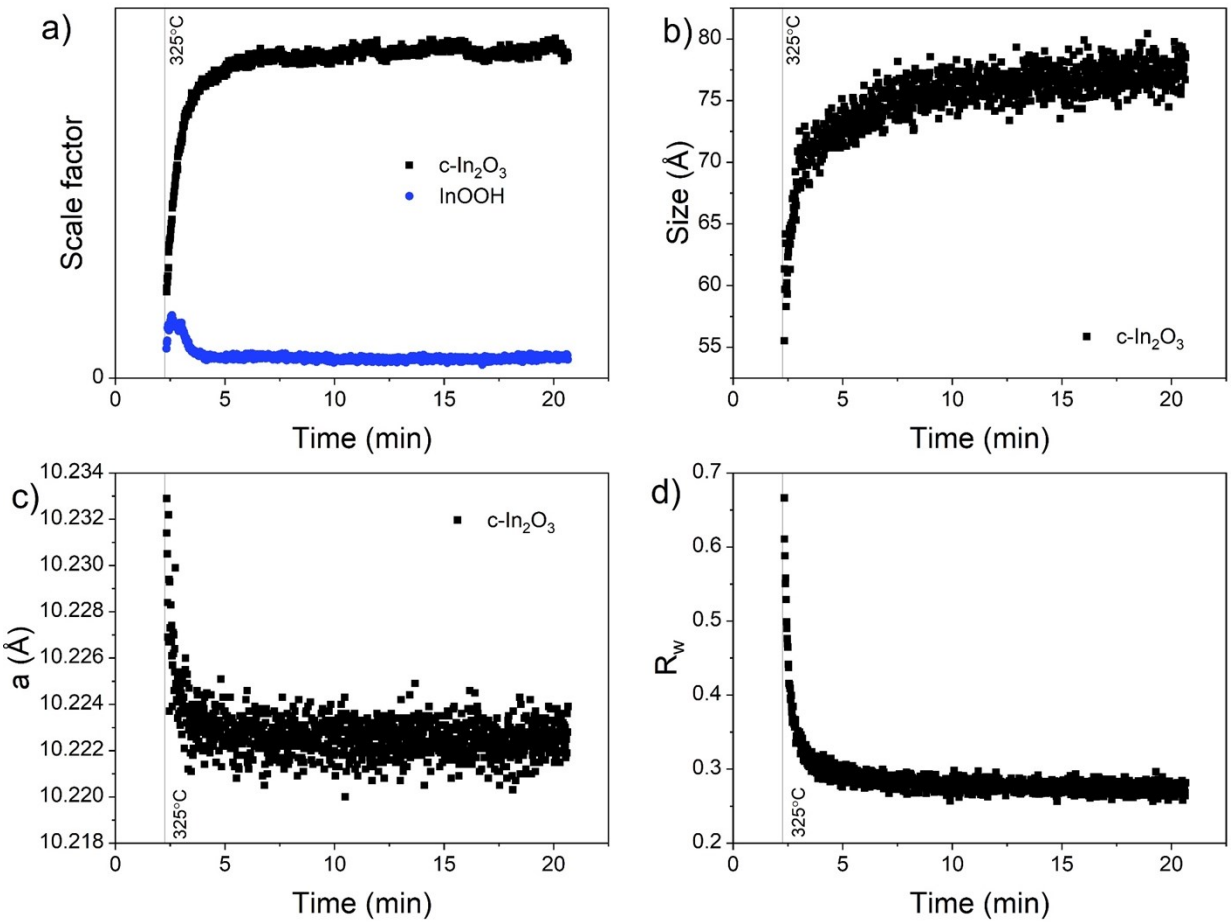

Figure S27. Extracted parameters from PDF analysis of W325 (Solvent: Water, Heating: Direct to 325 °C). a) Scale factors. b) Sizes. c) Unit cell parameter, a. d) R-value.

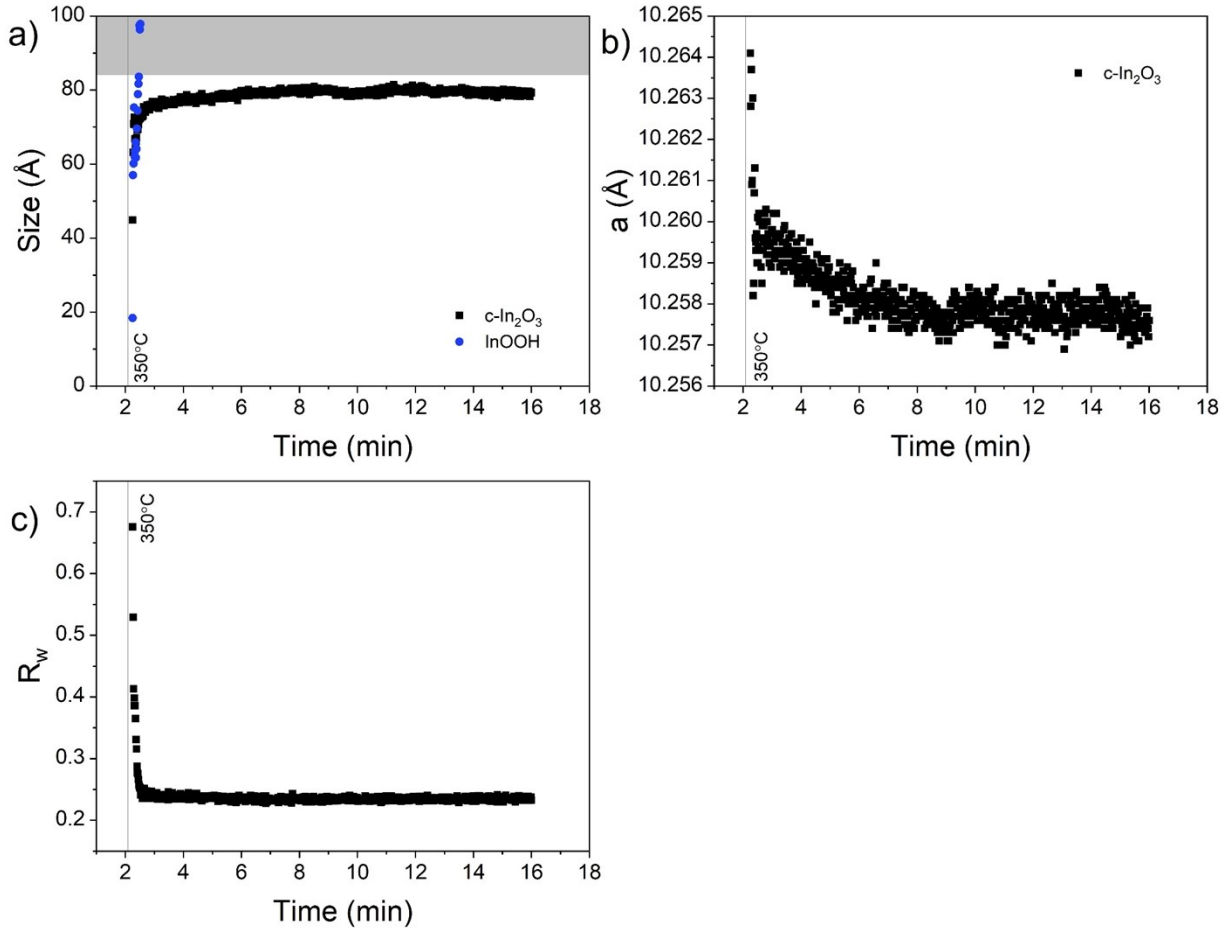

Figure S28. Extracted parameters from PDF analysis of W350 (Solvent: Water, Heating: Direct to 350 °C). a) Size (The grey area marks the approximate resolution limit, as defined by Sommer *et al.*[15] as where the Q_{damp} and size functions intersect. For the Q_{damp}=0.0349 as used here, the resolution limit is 84 Å). b) Unit cell parameter, a. c) R-value.

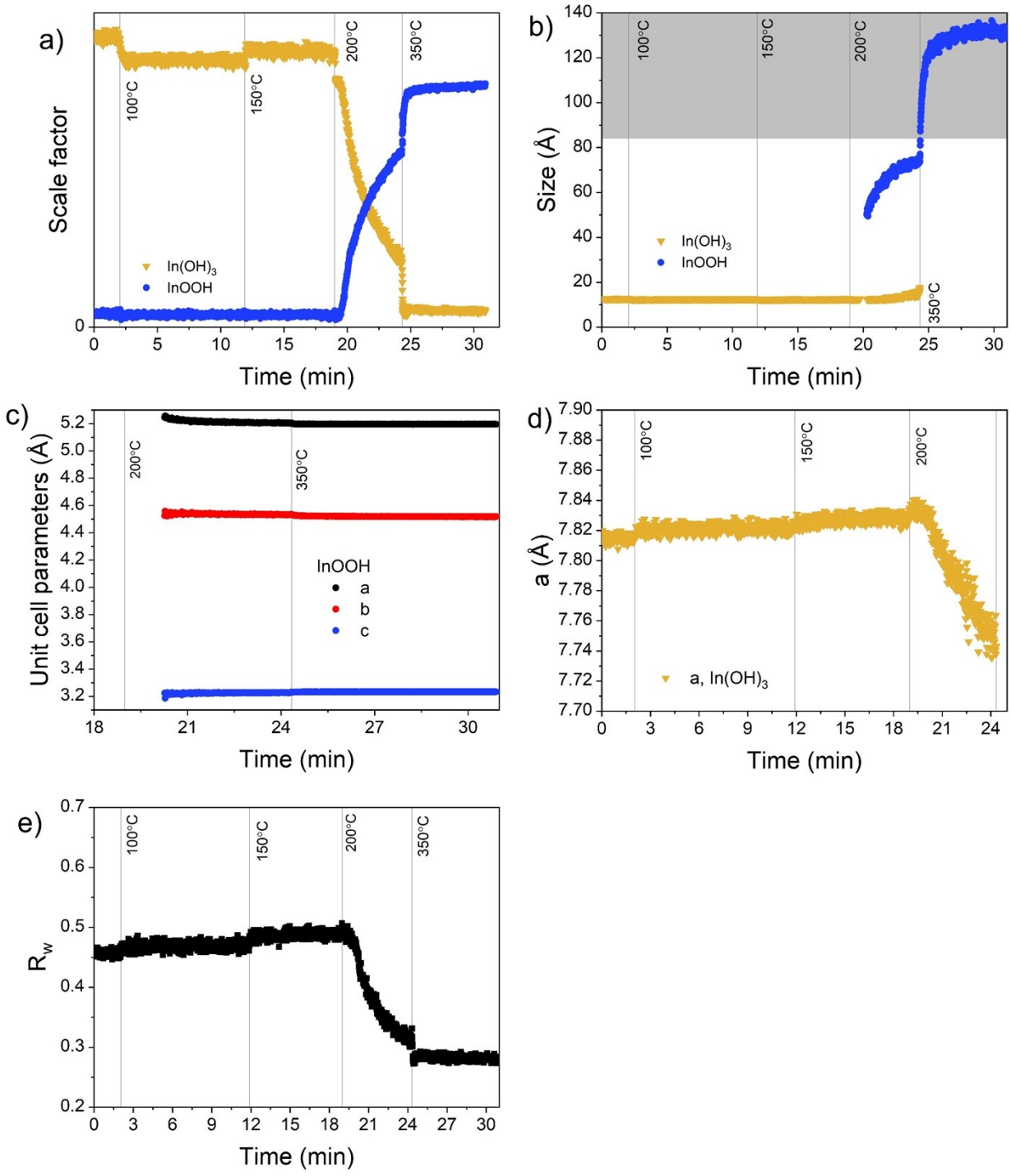

Figure S29. Extracted parameters from PDF analysis of WBRamp1 (Solvent: Water with added NaOH, Heating: Ramp with steps at 100, 150, 200 and 350 °C). a) Scale factors. b) Sizes (The grey area marks the approximate resolution limit, as defined by Sommer *et al.*[15] as where the Q_{damp} and size functions intersect. For the Q_{damp}=0.0349 as used here, the resolution limit is 84 Å). c) Unit cell parameters for InOOH. d) Unit cell parameters for $In(OH)_3$. e) R-value.

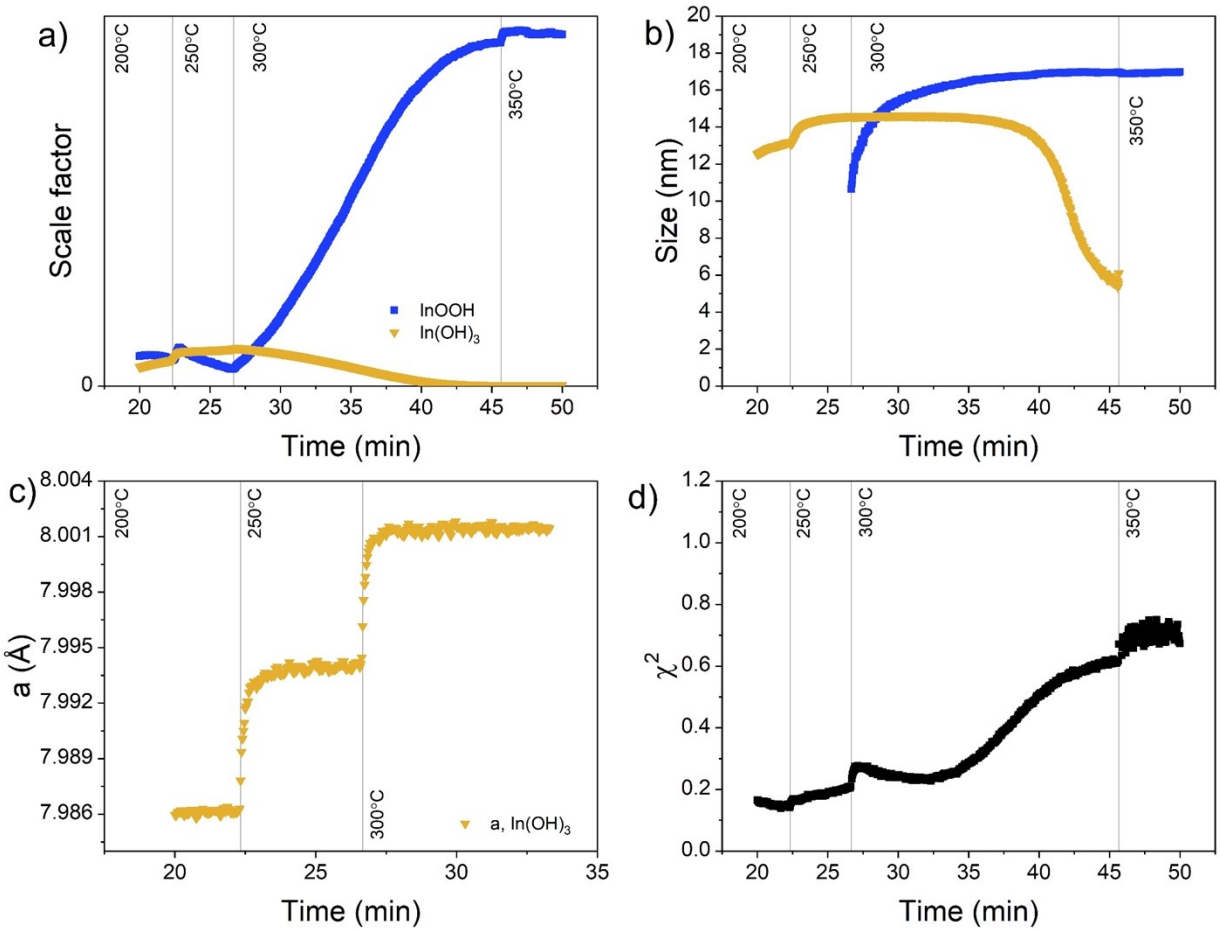

Figure S30. Extracted parameters from Rietveld refinement of WBRamp2 (Solvent: Water with added NaOH, Heating: Ramp with steps at 100, 150, 200, 250, 300 and 350 °C). a) Extracted scale factors. b) Extracted sizes. c) Unit cell parameters. d) χ^2-value.

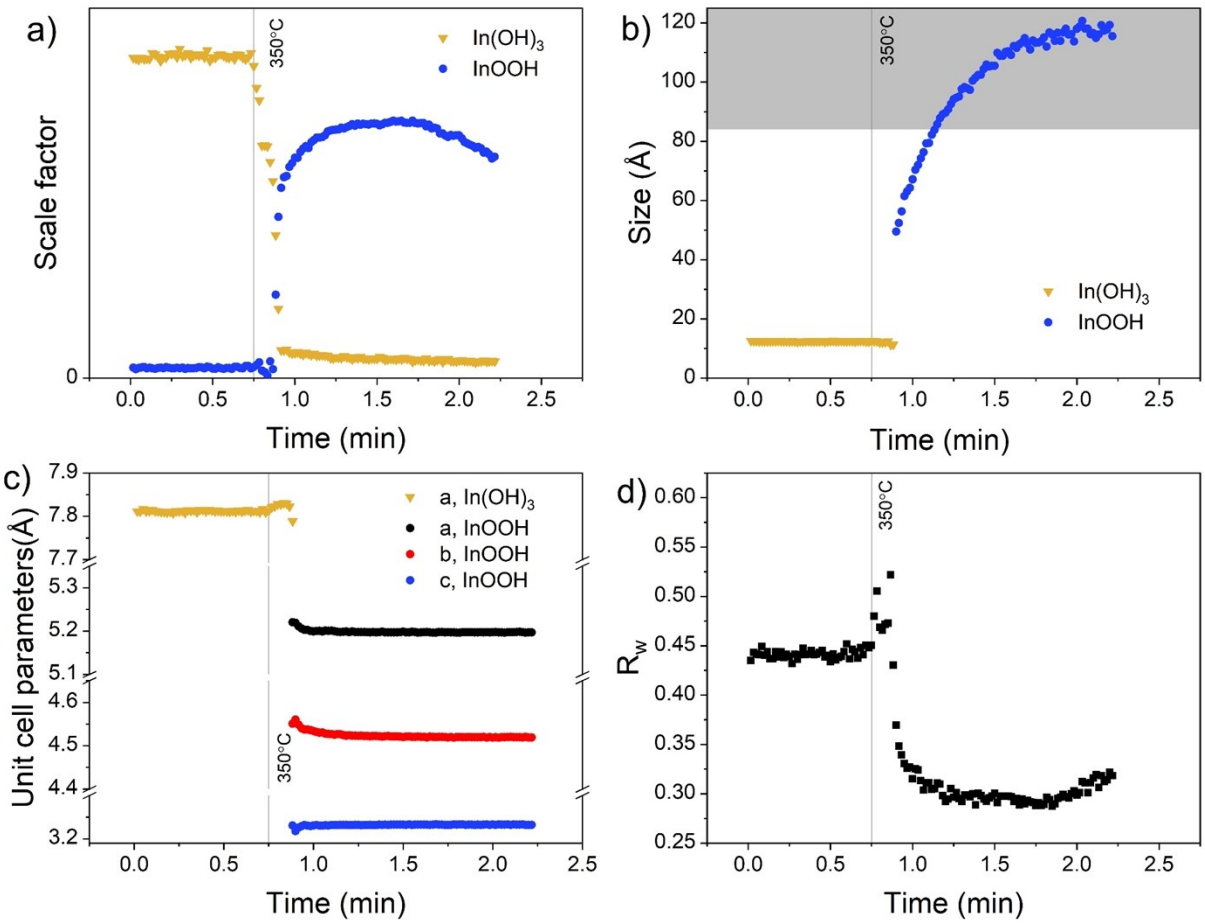

Figure S31. Extracted parameters from PDF analysis of WB350 (Solvent: Water with added NaOH, Heating: Direct to 350 °C). a) Scale factors. b) Sizes (The grey area marks the approximate resolution limit, as defined by Sommer *et al*.[15] as where the Q_{damp} and size functions intersect. For the Q_{damp}=0.0349 as used here, the resolution limit is 84 Å). c) Unit cell parameters. d) R-value.

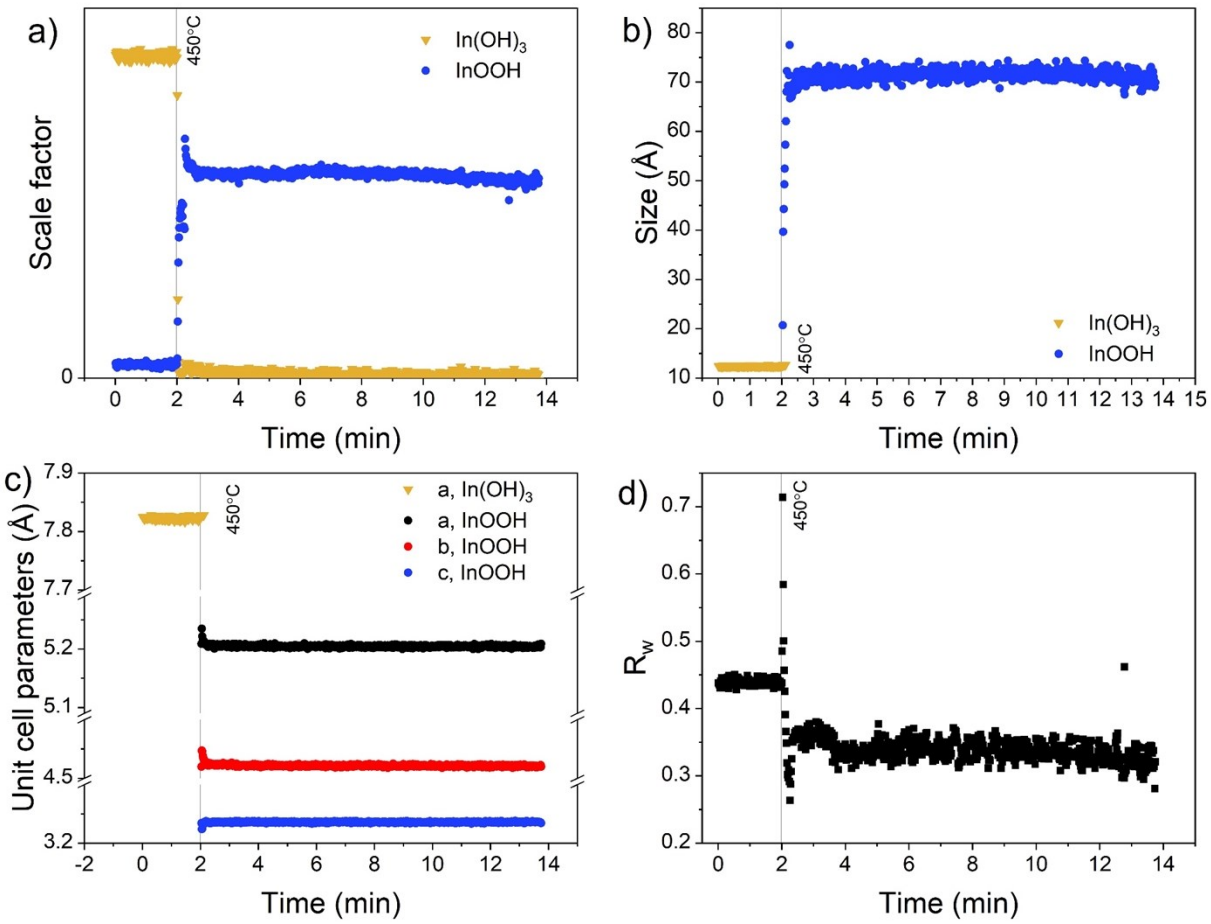

Figure S32. Extracted parameters from PDF analysis of WB450 (Solvent: Water with added NaOH, Heating: Direct to 450 °C). a) Scale factors. b) Sizes. c) Unit cell parameters. d) R-value.

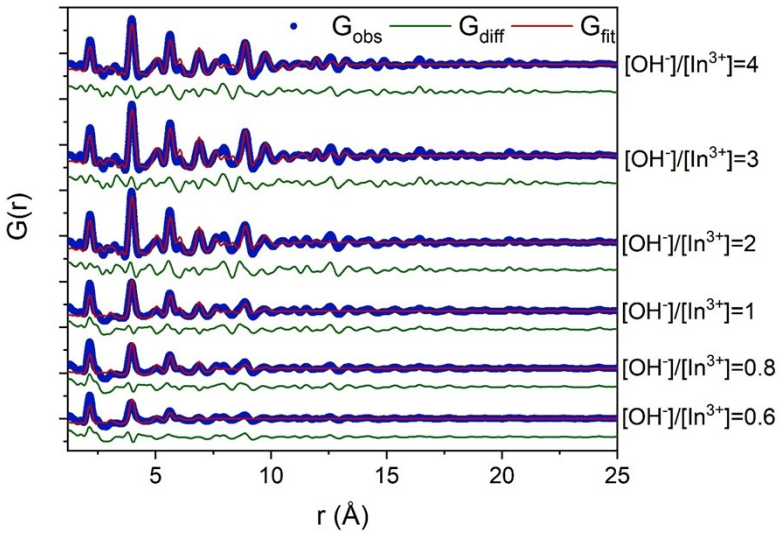

Figure S33. PDF analysis of solutions of In^{3+} with added NaOH in different ratios.

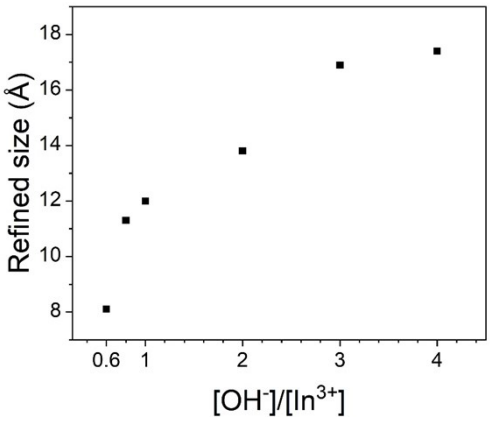

Figure S34. Extracted sizes from the PDF analysis of solutions of In^{3+} with added NaOH in different ratios.

			c-In_2O_3				InOOH					h-In_2O_3				$In(OH)_3$						
Concentration /M	Solvent	Temperature /°C	Scale	a	Y	Ig	Scale	a	b	c	Y	Scale	a	c	Y	Scale	a	Y	Rp	Rwp	Re	chi
0.01	H_2O	325					0.03827	5.30363	4.58165	3.24281	1.08662								22.8	28.7	5.65	25.82
0.01	H_2O	350					0.03799	5.29829	4.57854	3.25375	0.87625								23.9	29.1	5.36	29.49
0.01	H_2O	375					0.02908	5.28951	4.57782	3.25852	0.75927								24.4	28.9	6.18	21.82
0.01	H_2O	400	1.51E-06	10.1093	0.23358		0.02557	5.28095	4.57819	3.26355	0.62965								26.4	29.9	6.59	20.55
0.01	H_2O	425	2.91E-06	10.1093	0.23358		0.0221	5.28199	4.57589	3.26177	0.6675								27.3	30.8	7.16	18.58
0.01	H_2O	450	4.40E-04	10.1174	0.13088		0.02436	5.28531	4.57767	3.2636	0.67928								26.8	30.8	6.67	21.27
0.01	H_2O	200					0.02823	5.34807	4.59664	3.24281	1.31229					1.29E-05	7.97066	0.12433	27.2	34	6.28	29.26
0.01	EtOH	325	9.21E-05	10.105	0.38947	0.00944	0.04066	5.26 (F)	4.59 (F)	3.27 (F)	1.96661								14.1	18.1	4.32	18.21
0.01	EtOH	350	1.41E-04	10.1252	0.24093	0.01381	0.00827	5.26 (F)	4.59 (F)	3.27 (F)	1.32275								13.6	15.7	5.43	8.376
0.01	EtOH	375	2.63E-04	10.1236	0.18855	0.01291						1.73E-04	5.4858	14.507	0.18844				8.4	10	4.22	5.662
0.01	EtOH	400	2.62E-04	10.1223	0.18479	0.01819						1.73E-04	5.48514	14.5044	0.21467				7.88	9.49	4.23	5.035
0.01	EtOH	425	2.61E-04	10.1237	0.18214	0.02267						7.29E-05	5.48537	14.508	0.23971				7.68	9.2	4.33	4.51
0.01	EtOH	450	2.17E-04	10.1263	0.17592	0.02476						2.40E-05	5.48779	14.5034	0.21797				13.5	15	4.79	9.774
0.01	EtOH	200	1.83E-07	10.0682 (F)	0.31927 (F)	0.02008 (F)	0.03398	5.26 (F)	4.59 (F)	3.27 (F)	1.7683								21.3	26.9	5.85	21.19
0.01	EtOH	250	9.24E-06	10.0682	0.31927	0.02008	0.05123	5.26 (F)	4.59 (F)	3.27 (F)	1.76105								16.7	21	4.4	22.78
0.1	EtOH	350	1.31E-04	10.132	0.27587	0.00636	0.0028	5.26 (F)	4.59 (F)	3.27 (F)	0.92916								13.5	15	4.79	9.774
0.5	EtOH	350	9.74E-05	10.1334	0.23671	0.01436	0.00216	5.26 (F)	4.59 (F)	3.27 (F)	0.62202								11	13.3	6.82	3.806
1	EtOH	350	9.58E-05	10.1351	0.20315	0.0092	0.00127	5.26 (F)	4.59 (F)	3.27 (F)	0.63055								11.4	13.4	7	3.69

Table S8. Extracted values of all parameters refined during Rietveld refinement for flow synthesized samples.

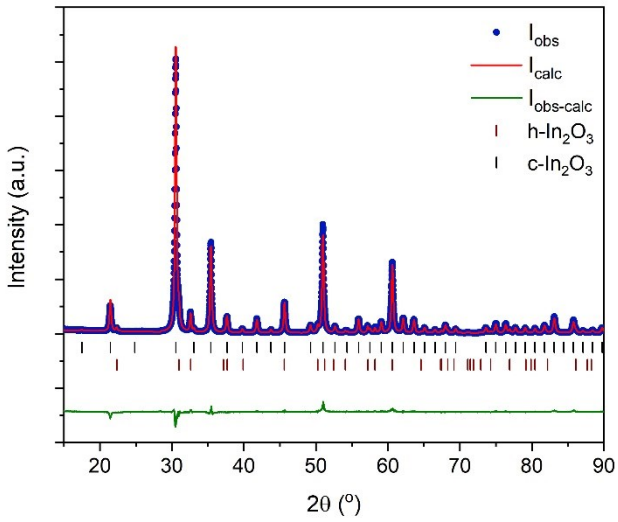

Figure S35. Rietveld refinement with c-In_2O_3 and h-In_2O_3 for the sample synthesized by flow at 375 °C in ethanol.

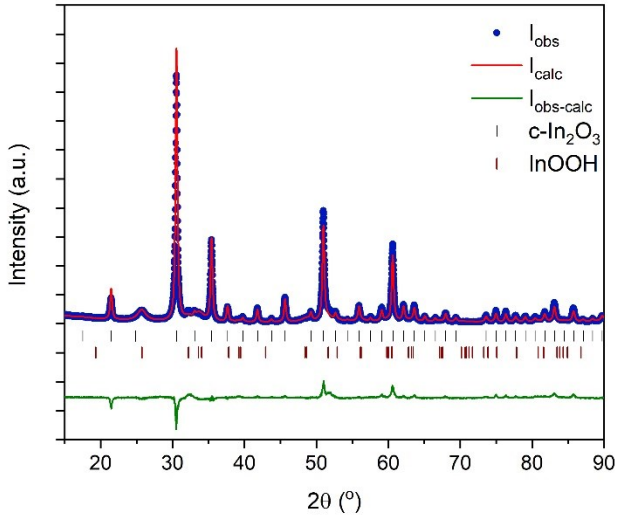

Figure S36. Rietveld refinement with c-In_2O_3 and InOOH for the sample synthesized by flow at 350 °C in ethanol.

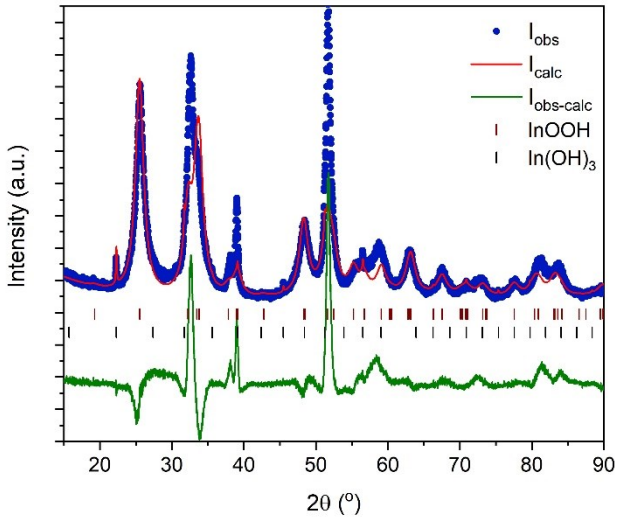

Figure S37. Rietveld refinement with $In(OH)_3$ and InOOH for the sample synthesized by flow at 200 °C in water.

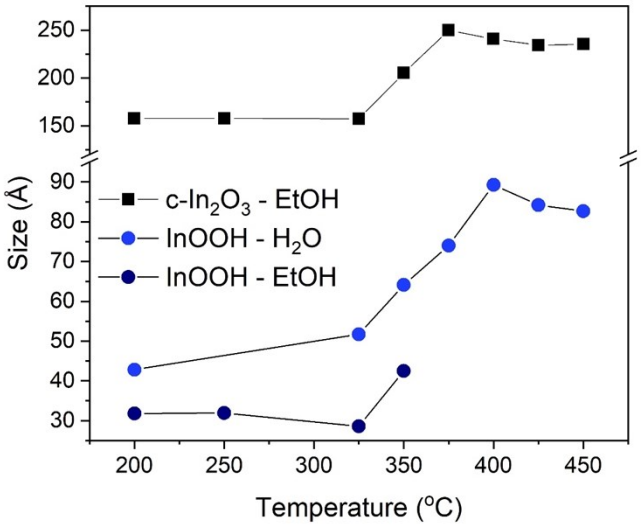

Figure S38. Refined crystallite sizes for the flow samples. The uncertainties are smaller than the symbols and are provided by the FullProf software.

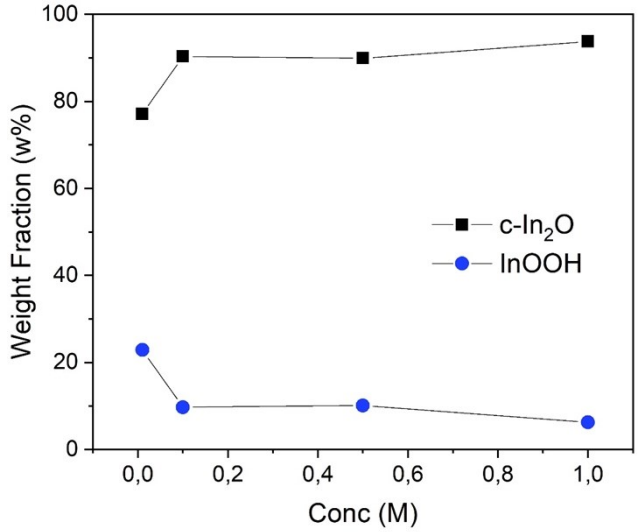

Figure S39. Extracted weight fractions for the concentration series synthesized by flow at a temperature of 350 °C. The uncertainties are smaller than the symbols and are provided by the FullProf software.

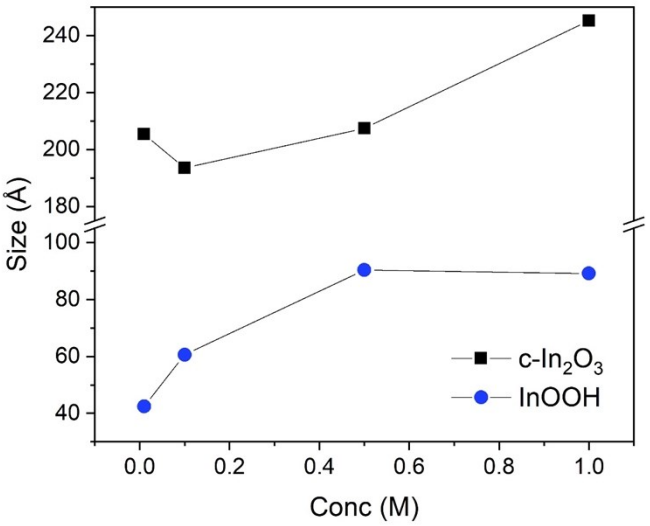

Figure S40. Extracted crystallite sizes for the concentration series synthesized by flow at a temperature of 350 °C. The uncertainties are smaller than the symbols and are provided by the FullProf software.

		$In(OH)_3$				$c\text{-}In_2O_3$							
Sample	Preparation	Scale	a	X	Ig	Scale	a	Y	Ig	Rp	Rwp	Re	chi
$In(OH)_3$	As synthesized in autoclave	6.275E-4	7.96456	5.22429E-2	5.54839E-3					17.9	23.2	4.31	29.0
$c\text{-}In_2O_3$	After STA to 380 °C					0.18253E-04	10.12006	0.180499	0.11154E-1	23.9	24.7	10.53	5.49

Table S9. Values from Rietveld refinement of PXRD data of the autoclave synthesized $In(OH)_3$ as well as the resulting product after STA to 380 °C.

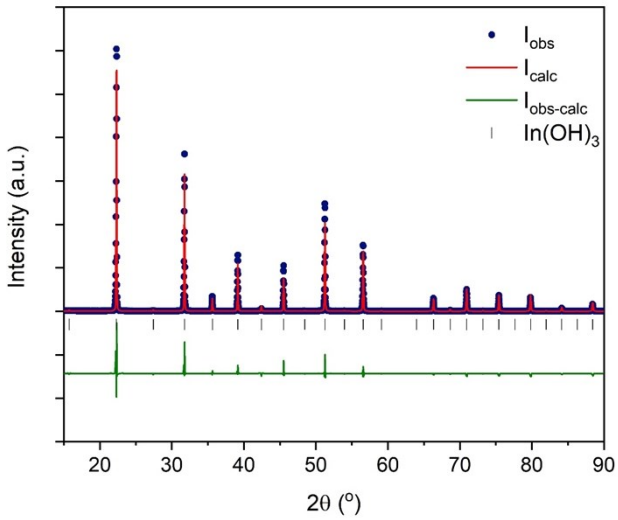

Figure S41. Rietveld refinement of PXRD for the autoclave synthesized $In(OH)_3$. The size broadening is not possible to refine as it is smaller than the instrumental broadening (size >100 nm).

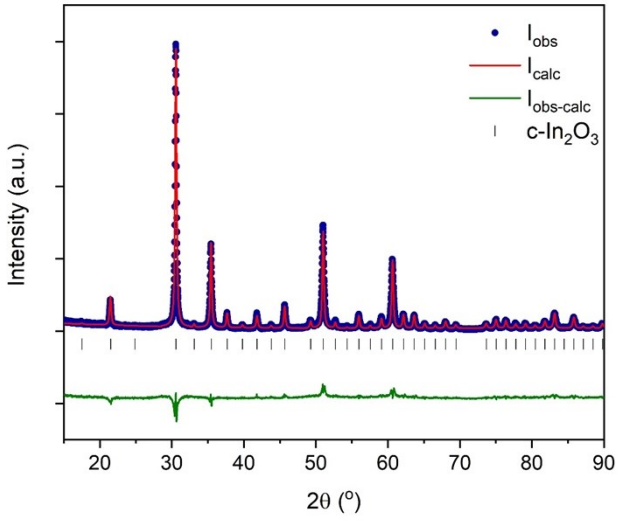

Figure S42. Rietveld refinement of PXRD of the $In(OH)_3$ sample after calcination at 380 °C with a $c\text{-}In_2O_3$ phase. The refined size is 26 nm.

	InOOH					h-In_2O_3								
Temperature / °C	Scale	a	b	c	Y	Scale	a	c	Y	Ig	Rp	Rwp	Re	chi
320	1.221E-3	5.31329	4.59572	3.2452	0.37812						18.9	26.0	4.17	38.8
410						2.698E-05	5.46636	14.4891	0.020817	0.144866	35.6	36.1	5.06	51.1

Table S10. Values from Rietveld refinement of PXRD data from the *in situ* calcination of InOOH. The diffractograms from which the values are extracted are the ones just before and after the observed transformation.

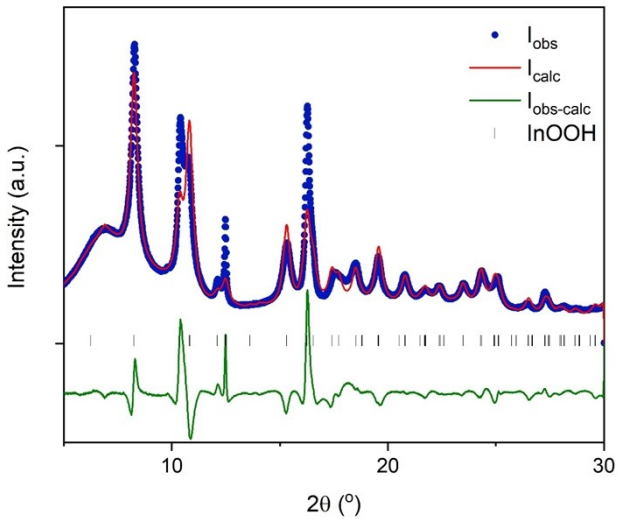

Figure S43. Rietveld refinement of InOOH at 320 °C during the *in situ* calcination experiment, with an isotropic size model. The refined size is 4.8 nm.

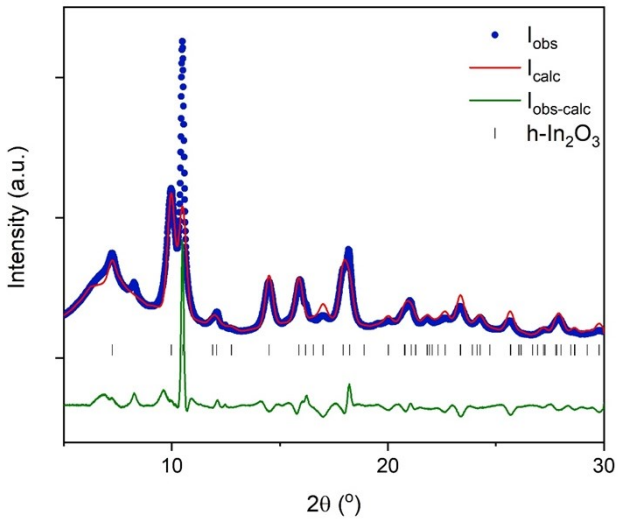

Figure S44. Rietveld refinement of h-In_2O_3 at 410 °C during the *in situ* calcination experiment, with an isotropic size model. The refined size is 6.7 nm.

Refinement of flow synthesized InOOH

As observed in Figure S37 and S40 the Rietveld refinements of InOOH-rich samples synthesized by flow with water as solvent have high residuals in contrast to the InOOH samples synthesized during *in situ* solvothermal experiments (Figure S20).

A phase pure InOOH sample (synthesized in flow at 325 °C with water as solvent) was further investigated. Using TS and PDF analysis a satisfactory fit was obtained (Figure S45), confirming that the atomic structure is InOOH. On the contrary, PXRD data measured both in house and at synchrotron both result in unsatisfactory fits. Both of the datasets have matching relative peak intensities and widths (Figure S46). This suggest the PXRD data are representative for the sample. The higher quality synchrotron data was used to test numerous models (Table S11). To confirm the unit cell parameters, a Le Bail refinement was employed. Using an anisotropic size model with 3 spherical harmonics both peak positions and the peak shapes are well described. Rietveld refinement using the anisotropic size model still had substantial undescribed intensity. A refinement including preferred orientation was observed to further improve the fit (Figure S45), while a large residual was still observed. Refinement of other parameters such as the atomic sites, occupancy and thermal motion of indium was also attempted without yielding better descriptions of the data.

TEM images of the sample show highly agglomerated small crystallites, which are slightly elongated and possibly plate like (Figure S48). As the PXRD patterns are similar when measured with a flat sample holder (in house/Bragg-Brentano geometry) and spinning capillary (synchrotron/Debye-Scherrer geometry) a high degree of preferred orientation is not expected in the system (Figure S46).

As preferred orientation and anisotropic size broadening cannot fully described data we suggest that defects in the structure might also contribute to the unexplained intensities.

High residuals are also observed when refining h-In_2O_3 calcined from InOOH as observed in Figure S44. In Figure S49 the measured diffractograms of InOOH and h-In_2O_3 originating from InOOH are compared to reference diffractograms. These clearly show that the relative intensities in both cases does not match the references. This indicate that the effect, which cannot be modelled for InOOH, is transferred into h-In_2O_3. This observation correspond well with the proposed transformation mechanism from InOOH to h-In_2O_3.

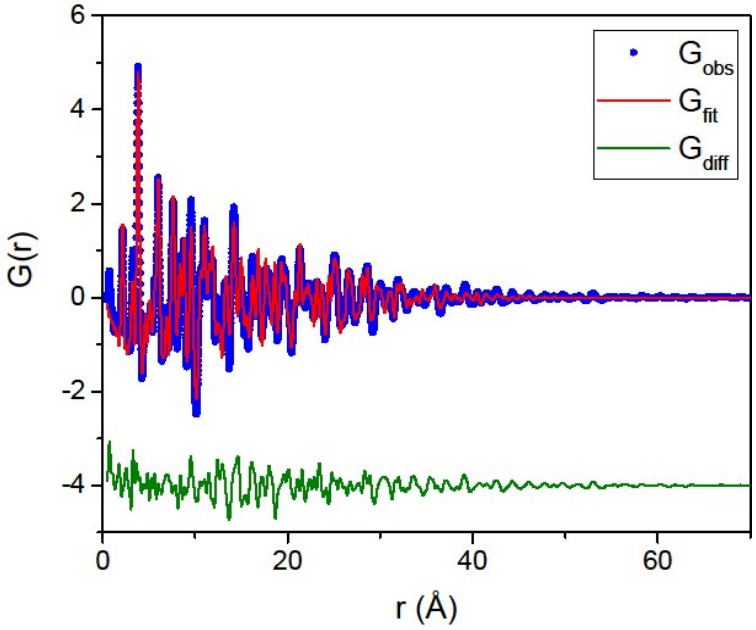

Figure S45. PDF analysis of the InOOH sample synthesized by flow with water as solvent and a temperature of 325 °C.

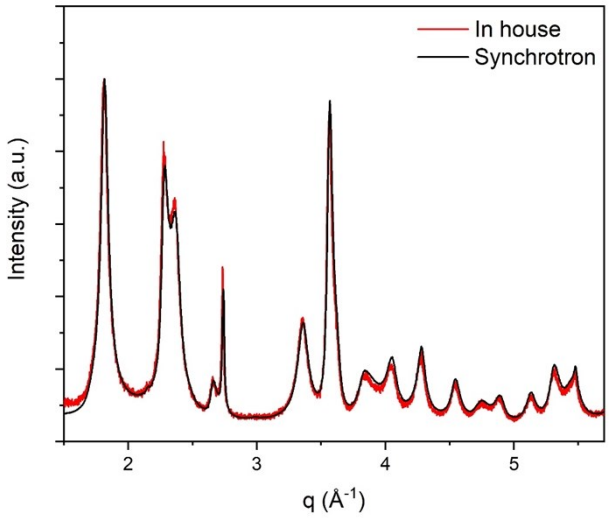

Figure S46. Comparison of PXRD of the InOOH sample measured in house and at Spring8 synchrotron.

Model	Method	Rp	Rwp	Re	chi
Isotropic size	Rietveld	19.8	26.1	1.5	302
3 Spherical harmonics	Rietveld	18.9	24.8	1.49	275.5
3 Spherical harmonics and Preferred orientation	Rietveld	18.4	23.0	1.52	228.4
Isotropic size	Le Bail	12.6	15.7	1.5	108.9
3 Spherical harmonics	Le Bail	9.43	12.6	1.39	82.62

Table S11. R-values for the different models refined against the PXRD data

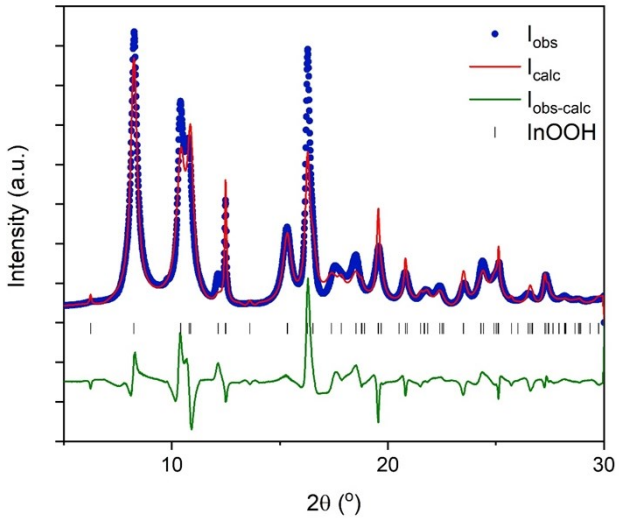

Figure S47. Rietveld refinement of InOOH sample with size broadening modelled by 3 spherical harmonics and preferred orientation modelled by the March-Dollase Numeric Multiaxial Function with [101] and [010]. The model is not satisfactory, but shown as it is the best obtained fit to the data.

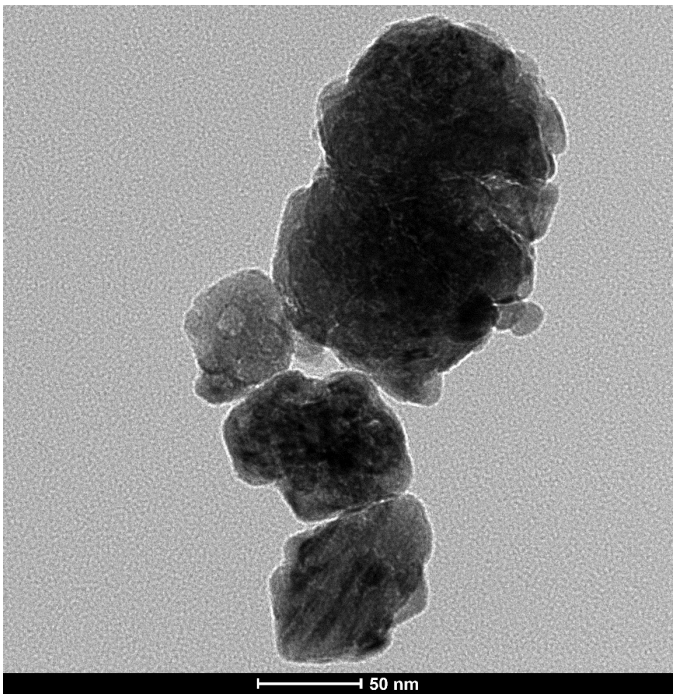

Figure S48. TEM image of the InOOH sample synthesized by flow with water as solvent and a temperature of 325 °C. The image is considered representative of the observed particles

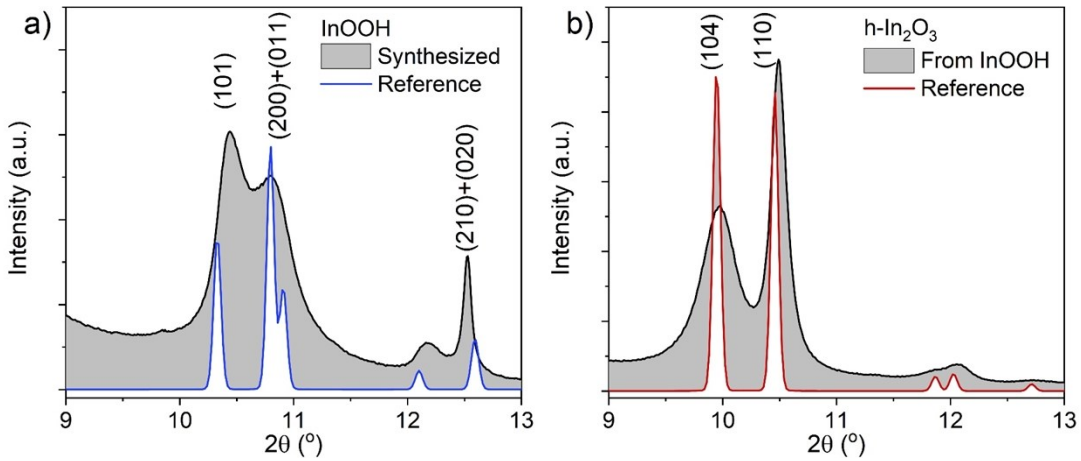

Figure S49. Comparison of the measured PXRD data to diffractograms calculated from reference systems.[16,17]

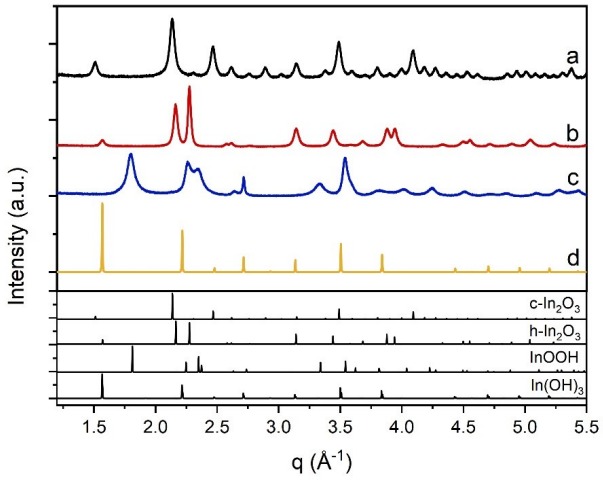

Figure S50. PXRD of phase pure synthesis products. a) c-In_2O_3 synthesized by continuous flow synthesis at 450°C with ethanol as solvent. b) h-In_2O_3 synthesized by calcination of dry InOOH powder at 600°C. c) InOOH synthesized by continuous flow synthesis at 325°C with water as solvent. d) $In(OH)_3$ synthesized in autoclave at 140°C with water as solvent and addition of NaOH.

References

1 Z. Fang, H. Assaaoudi, R. I. L. Guthrie, J. A. Kozinski and I. S. Butler, Continuous Synthesis of Tin and Indium Oxide Nanoparticles in Sub- and Supercritical Water, *J. Am. Ceram. Soc.*, 2007, **90**, 2367–2371.

2 S. Elouali, L. G. Bloor, R. Binions, I. P. Parkin, C. J. Carmalt and J. A. Darr, Gas Sensing with Nano-Indium Oxides (In_2O_3) Prepared via Continuous Hydrothermal Flow Synthesis, *Langmuir*, 2012, **28**, 1879–1885.
3 A. J. T. Naik, R. Gruar, C. J. Tighe, I. P. Parkin, J. A. Darr and R. Binions, Environmental sensing semiconducting nanoceramics made using a continuous hydrothermal synthesis pilot plant, *Sens. Actuator, B*, 2015, **217**, 136–145.
4 M. Niederberger, G. Garnweitner, J. Buha, J. Polleux, J. Ba and N. Pinna, Nonaqueous synthesis of metal oxide nanoparticles:Review and indium oxide as case study for the dependence of particle morphology on precursors and solvents, *J. Sol-Gel Sci. Technol.*, 2006, **40**, 259–266.
5 X. Tao, Y. Zhao, L. Sun and S. Zhou, One-pot low temperature solvothermal synthesis of In_2O_3 and InOOH nanostructures, *Mater. Chem. Phys.*, 2015, **149**, 275–281.
6 L. Schlicker, M. F. Bekheet and A. Gurlo, Scaled-up solvothermal synthesis of nanosized metastable indium oxyhydroxide (InOOH) and corundum-type rhombohedral indium oxide (rh-In_2O_3), *Z. Kristallogr. - Cryst. Mater.*, 2017, **232**, 129–140.
7 D. B. Yu, D. B. Wang and Y. T. Qian, Synthesis of metastable hexagonal In_2O_3 nanocrystals by a precursor-dehydration route under ambient pressure, *J. Solid State Chem.*, 2004, **177**, 1230–1234.
8 T. Yan, X. Wang, J. Long, H. Lin, R. Yuan, W. Dai, Z. Li and X. Fu, Controlled preparation of In_2O_3, InOOH and $In(OH)_3$ via a one-pot aqueous solvothermal route, *New J. Chem.*, 2008, **32**, 1843–1846.
9 L.-Y. Chen, Z.-X. Wang and Z.-D. Zhang, Corundum-type tubular and rod-like In_2O_3 nanocrystals: synthesis from designed InOOH and application in photocatalysis, *New J. Chem.*, 2009, **33**, 1109–1115.
10 S. E. Lin and W. C. J. Wei, Synthesis and growth kinetics of monodispersive indium hydrate particles, *J. Am. Ceram. Soc.*, 2006, **89**, 527–533.
11 V. D. Ashok and S. K. De, Growth Kinetics of Self-Assembled Indium Hydroxide and Oxide in Electrolytic Alkali Halide Solution, *J. Phys. Chem. C*, 2011, **115**, 9382–9392.
12 C. Shifu, Y. Xiaoling, Z. Huaye and L. Wei, Preparation, characterization and activity evaluation of heterostructure $In_2O_3/In(OH)_3$ photocatalyst, *J. Hazard. Mater.*, 2010, **180**, 735–740.
13 M. Epifani, P. Siciliano, A. Gurlo, N. Barsan and U. Weimar, Ambient Pressure Synthesis of Corundum-Type In_2O_3, *J. Am. Chem. Soc.*, 2004, **126**, 4078–4079.
14 D. Chu, Y.-P. Zeng, D. Jiang and J. Xu, Tuning the phase and morphology of In_2O_3 nanocrystals via simple solution routes, *Nanotechnology*, 2007, **18**, 435605.
15 S. Sommer, I. G. Nielsen and B. B. Iversen, Reliability of the Pair Distribution Function across in situ experiments and data processing, *In preparation*.
16 M. S. Lehmann, F. K. Larsen, F. R. Poulsen, A. N. Christensen and S. E. Rasmussen, Neutron and X-Ray Crystallographic Studies on Indium Oxide Hydroxide, *Acta Chem. Scand.*, 1970, **24**, 1662–1670.
17 C. T. Prewitt, R. D. Shannon, D. B. Rogers and A. W. Sleight, C rare earth oxide-corundum transition and crystal chemistry of oxides having the corundum structure, *Inorg. Chem.*, 1969, **8**, 1985–1993.